Natural Resources Canada
Ressources naturelles Canada

GEOLOGICAL SURVEY OF CANADA
OPEN FILE 8986

Permafrost-related landforms and geotechnical data compilation, Yellowknife to Grays Bay corridor region, Slave geological province

P.D. Morse, R.J.H. Parker, S.L. Smith, and W.E. Sladen

2023

Canada

GEOLOGICAL SURVEY OF CANADA
OPEN FILE 8986

Permafrost-related landforms and geotechnical data compilation, Yellowknife to Grays Bay corridor region, Slave geological province

P.D. Morse, R.J.H. Parker, S.L. Smith, and W.E. Sladen

2023

Permanent link: https://doi.org/10.4095/332017

This publication is available for free download through GEOSCAN (https://geoscan.nrcan.gc.ca/).

Recommended citation
Morse. P.D., Parker, R.J.H., Smith, S.L., and Sladen, W.E., 2023. Permafrost-related landforms and geotechnical data compilation, Yellowknife to Grays Bay corridor region, Slave geological province; Geological Survey of Canada, Open File 8986, 1 .zip file. https://doi.org/10.4095/332017

Publications in this series have not been edited; they are released as submitted by the author.

ISSN 2816-7155
ISBN 978-0-660-49422-7
Catalogue No. M183-2/8986E-PDF

ABSTRACT

Permafrost conditions in the Slave Geological province are not well understood. Thaw of permafrost and associated ground ice can reduce ground stability, which modifies terrain and drainage patterns and affects terrestrial and aquatic ecosystems. This presents critical challenges to northern resource development and societies where thaw of ice-rich permafrost negatively affects the integrity of ground-based infrastructure. In an effort to address this knowledge gap, this report presents a digital georeferenced database of landforms identified in permafrost terrain using high-resolution satellite imagery and provides information on geomorphic indicators of ground ice presence and thaw susceptibility. Digital georeferenced databases compiled from sedimentological and cryostratigraphic records are also provided. The landform database is focused on mapping within a 10 km-wide swath of land (8576 km^2 area of interest) centred on the proposed corridors for the 773 km-long Slave Geological Province Corridor Project, NT, and the Grays Bay Road and Port Project, NU. The geomorphic features were classified and digitized using high-resolution (0.5 m) satellite imagery following an existing protocol, which was modified by using a very high-resolution (2 m) digital elevation model (DEM), and by including mapping criteria for additional features. A total of 1393 geomorphic features were mapped comprising 10 different types, which were categorized into 3 classes that include periglacial (1291), hydrological (88), and mass movement (14) features. Data from 254 geotechnical boreholes and 2243 granular deposits were compiled. Information from the compiled databases was analyzed with surficial geology information. Results indicate that the distributions and densities of mapped landforms varied substantially according to surficial geology. High ground ice contents may be quite common in glaciofluvial deposits where creep of frozen ground affects about 30% of eskers. And ground ice may be more extensive overall than the available geotechnical data indicate. Borehole and granular deposit data suggest that overburden thickness above bedrock was up to 25.5 m, and visible ground ice contents were generally between 10% and 30%, but were up to 60% in glacial blanket and glaciofluvial sediments.

DISCLAIMER

Table of Contents

List of Figures

List of Tables

1 Introduction

The Slave Geological Province (Figure 1), has rich mineral resources (CIRNAC et al., 2021), great northern economic development potential, and is the location of the proposed Slave Geological Province Corridor Project and the Grays Bay Road and Port Project. Glaciated in the Late Wisconsinan, permafrost ranges from extensive discontinuous in the south to continuous in the north of this region (Heginbottom et al., 1995), and is associated with extensive thaw-stable bedrock outcrops and unconsolidated surficial deposits where the landscape stability is achieved through ice-bonding of sediments. Surficial deposits are dominated by till and glaciofluvial sediments, whereas raised post-glacial marine sediments are abundant below about 200 m asl in the north at the coast of Coronation Gulf (Geological Survey of Canada, 2017a, 2017b, 2016a, 2016b, 2015, 2014a, 2014b; Kerr, 2018, 2014; Olthof et al., 2014; Stevens et al., 2017 Wolfe et al., 2017). The thaw sensitivity of these sediments is strongly related to ground temperature, materials, and ice content, but this information is sparse and much of it is located exclusively in hard copy reports that are difficult to attain.

The purpose of this report is to present results from the first regional-scale approach to map permafrost-related landforms in the Slave Geological Province, together with a compilation of sedimentological and cryostratigraphic records for this region that have been extracted from available reports. The objectives of this study are to: i) identify and classify various permafrost-related landforms using high-resolution satellite imagery acquired for a 10-km-wide swath of land (8576 km^2 area of interest) aligned with the proposed corridors for the Slave Geological Province Corridor Project, NT, and the Grays Bay Road and Port Project, NU ; ii) provide quantitative measures of the distributions and densities of the set of landforms and determine their associations with surficial geology; and iii) identify and digitally compile the data from available sedimentological and cryostratigraphic records to increase its utility and accessibility. This knowledge on thaw-sensitive permafrost conditions is needed to inform decisions regarding development of resources and climate-resilient northern infrastructure, to identify potential geohazards, and to make inferences on past and future landscape evolution.

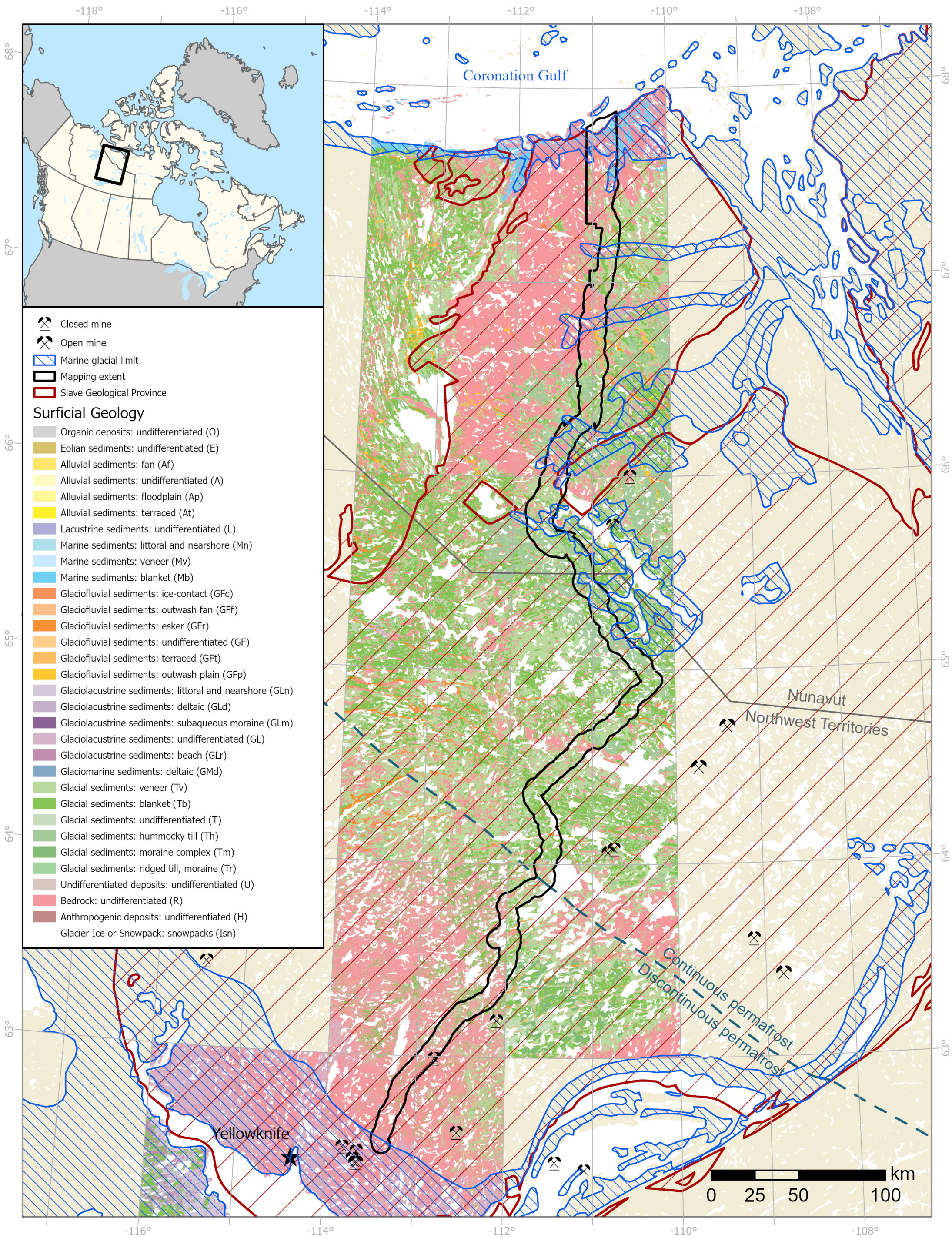

Figure 1. Location of the study area in the Slave Geological Province with respect to surficial geology and permafrost zone. The area of interest (AOI) is a 10-km wide swath that follows the proposed corridors for the Slave Geological Province Corridor Project in Northwest Territories and the Grays Bay Road and Port Project in Nunavut. The surficial geology legend follows the GSC Surficial Data model V2.3.14, and the symbology descriptions and codes are used throughout this report. The inset map show the location of the study area in the Canadian north. Surficial geology data are from Geological Survey of Canada (2017a, 2017b, 2016a, 2016b, 2015, 2014a, 2014b; Kerr, 2018, 2014; Olthof et al., 2014; Stevens et al., 2017 Wolfe et al., 2017).

2 Physiographic Context

This work focuses on a corridor that extends from the end of the Ingraham Trail (Northwest Territories Highway 4), northward to the Northwest Territories - Nunavut border near Contwoyto Lake, and onward to the shore of the Coronation Gulf approximately 180 km east of Kugluktuk (Figure 1). The climate of this region varies from cold-continental in the south to maritime arctic near the coast (Wolfe et al., 2017). Climatic data for this region is sparse, but 1981-2010 climate normal data (Environment Canada, 2022) for three stations indicates that mean annual air temperature decreases with elevation and increases with proximity to the coast and annual precipitation decreases with latitude and increases with elevation (Table 1).

Table 1. 1981-2010 climate normal data for the region (Environment Canada, 2022).

Site name	Location	Elevation m asl	MAST °C	Total precipitation (percent as snow) mm
Kugluktuk	67.8252° N, 115.0966° W	23	-4.3	247.2 (74%)
Lupin Mine site	65.7499° N, 111.2500° W	490	-10.9	298.5 (46%)
Yellowknife	62.4540° N, 114.3718° W	206	-10.4	288.6 (55%)

The corridor falls completely within the Bear-Slave Upland physiographic region and the Slave Geological province. The elevation of the of the region ranges from 650 m asl in the interior uplands near Contwoyto Lake to sea level at the coast of the Coronation Gulf. Relief varies between less than 10 m to 30 m although escarpments and ridges exceeding 50 m are present (Wolfe et al., 2017). The bedrock predominately consists of Archean gneisses, metavolcanic and metasedimentary rocks, and widespread gneissic–granitoid plutons (Helmstaedt, 2009; Padgham and Fyson, 1992; Wolfe et al., 2017). With one of the highest estimated mineral potentials in the world, the Slave Geological Province is populated by numerous active and abandoned mines for gold, diamond and base metal mines (Figure 1), and major identified deposits of metals including lithium, cobalt and bismuth required for clean energy economies.

Deglaciation occurred approximately 10,500 BP and the region is still experiencing isostatic uplift (Kerr, 1996). Surficial materials of glacial origin are prevalent (Figure 1), but large areas of exposed bedrock are common in many localities. Near the Coronation Gulf, post-glacial marine sediments are also common below 200 m asl (Wolfe et al., 2017).

The distribution of permafrost in the study region varies from extensive discontinuous at more southerly locations to continuous permafrost at more northerly locations (Heginbottom et al., 1995). What little is known about in situ permafrost conditions is largely derived from a relatively small set of sedimentological and cryostratigraphic records (e.g., Kerr, 1996; Wolfe et al., 1997a). Permafrost-related landforms provide some insight about the relative ground ice content, thaw sensitivity, and geohazard potential, and this utility increases when landforms are linked to sedimentological and cryostratigraphic records and surficial geology. In this region, for example, Dredge et al. (1999) related surficial materials and landforms to ground ice conditions based upon records available at the time, and air photos have been used to assess the potential for mapping the presence of massive ice in granular deposits (AGRA Earth & Environmental Limited, 1998), but in each case, only at a limited number of sites were investigated. A review of the Slave Geological Province (Wolfe et al., 2017) indicates that at some locations, glacially-derived massive ground ice has been preserved in glaciogenic sediments, whereas at other locations segregated ice and ice-wedge polygons have formed in glaciomarine sediments and glaciofluvial deposits, respectively. A recent national-scale model (O'Neill et al., 2020) estimated that excess ice volume in the top 5 m of permafrost may be greater than 20-30% in some localities, but this estimate has not been validated. Although massive ground ice has only been observed at a few locations, landforms with geomorphological characteristics attributed to partial thawing and creep of ice-rich permafrost are regionally apparent (Wolfe et al., 2017).

3 Data and Methodology

The methodology utilized for identification and classification of geomorphic features closely follows those outlined by Sladen et al. (2021) and will not be described here in detail. However, some modifications necessary, such as those required to accommodate additional features, are described below.

3.1 Data

3.1.1 Satellite Imagery

Seventy-two high-resolution satellite image datasets (Appendix A) covering 8576 km^2 were processed and used to identify and digitize the extent of the features being mapped in this work. All but three datasets were acquired by the GeoEye-1, WorldView-2 or WorldView-3 satellites and delivered as 4-band or 8-band 2-m resolution multispectral image data paired with 0.5-m resolution panchromatic image data acquired at the same time. Two of the remaining three image datasets were WorldView-1 0.5-m resolution panchromatic image data and were pansharpened to improve mapping capability using 5-m resolution RapidEye multispectral image data that covered the same area. All satellite images were collected during snow free months under mostly clear skies.

3.1.2 Elevation Data

The elevation data were used to orthorectify the satellite imagery during processing, as well as to aid in image interpretation during the mapping procedure by providing context on the local relief. Elevation data were acquired from twelve mosaic tiles from ArcticDEM Release 7 (Porter et al., 2018). Each tile covers an area of 50 km by 50 km, has a pixel size of 2 x 2 m, and is referenced to the WGS84 ellipsoid. These data were projected to NAD 83 UTM Zone 12 N and used to convert the satellite imagery to 3D.

3.1.3 Geotechnical Data

A total of eleven reports were used to compile a geotechnical borehole database as well as two granular deposit databases. The data contained within the three databases describes the geotechnical conditions of various locations within the Slave Geological Province.

3.1.3.1 Geotechnical Borehole Data

The data from eleven geotechnical borehole reports, which were submitted in support of Environmental Assessments (BGC Engineering Inc., 2006a, 2006b; EBA Engineering Consultants Ltd., 1998, 1997, 1995a, 1993a; Golder Associates Ltd., 2001; SRK Consulting Engineers and Scientists, 2005, 2003, 2002; Wolfe et al., 1997), were compiled to provide context on the subsurface characteristics of the study area. The geotechnical borehole data was entered manually into Microsoft Excel spreadsheets and the structure follows that of other geotechnical databases published by the Geological Survey of Canada (Smith et al., 2005). Descriptions of the database fields not found in Smith et al. (2005) can be found in Appendix B Table B1.

Adequate location information was found for all boreholes except for those in EBA Engineering Consultants Ltd. (1993c) which used an unknown coordinate system. However, a map contained within the report had a grid referenced to the coordinate system and lake boundaries. This allowed the approximate georeferenced location of the boreholes to be set by “rubber sheeting” the map to the satellite imagery. Coordinates of a reference point placed in the georeferenced map at the intersection of north-south and east-west local grid lines were used to determine the spatial relation between the native format and UTM coordinates, and the offsets for the borehole locations were converted to UTM coordinates and added to the borehole database. The borehole locations in the database were converted into an ESRI® shapefile to allow for easier integration into GIS applications.

3.1.3.2 Granular Deposit Data

Information from three granular deposit assessment reports (EBA Engineering Consultants Ltd., 1993a; J.D. Mollard and Associates Ltd., 1993, 1994) for the region surrounding the mapping area was also compiled to provide context on the soil characteristics and landforms within the study area. EBA Engineering Consultants Ltd. (1993a) contained geotechnical information from granular test pits dug in various locations as well as descriptions of the landforms at specific locations, whereas the data reported by J.D. Mollard and Associates Ltd. (1993, 1994) only contained descriptions of the landforms at specific locations. These differences between the datasets necessitated the development of two databases (Appendix B Tables B2 and B3).

Each report was digitized using a combination of optical character recognition (OCR) and manual efforts. The reports were first converted to Microsoft Word or Excel formats using Adobe Acrobat's OCR and file conversion tools, and then the extracted data were manually reformatted into a structured Microsoft Excel database. The value of each cell in the database was then inspected and any transcription errors were corrected.

The coordinates in EBA Engineering Consultants Ltd. (1993a) and J.D. Mollard and Associates Ltd. (1994) were given in UTM, but the coordinates given in J.D. Mollard and Associates Ltd. (1993) were given as codes according to points on the military grid reference system (MGRS) (see "UTM GRID" in Figure 2) and referenced to the NAD27 datum. With the understanding that a MGRS grid is displayed in the UTM coordinate system (Natural Resources Canada, 2016), we converted the MGRS grid references to UTM coordinates, reprojected them from NAD27 to NAD83, and saved the coordinates in UTM format. It is important to note that the precision of the coordinates in J.D. Mollard and Associates Ltd. (1993) is to the closest 1000 m.

<u>"Mollard" database</u>

The Excel database was constructed with two tables. The "location" table contains the spatial information on each deposit, i.e the UTM zone and coordinates of the deposit, the NTS sheet code, and the deposit shape type (point, line, and polygon). Shape type was determined based on the number of points given to represent the deposit (Figure 2 Figure 3). The "description" table included the information on each deposit such as landform type, topography, relative size as well as information on the report the data was extracted from (Figure 4). Both tables are linked using the unique identifier (UID) code for each deposit, which is the combination of NTS sheet where the deposit sits and the deposit's prospect number. Descriptions of the database fields can be found in Appendix B Table B2.

The database was also converted into a set of ESRI shapefiles which represent the deposits as point, line, and polygon features depending upon the number of points (1, 2, 3+ respectively) used to describe the location of the deposit. Due to software limitations the polygon features are depicted as closed lines.

“EBA” database

EBA Engineering Consultants Ltd. (1993a) contained information on granular deposits including geotechnical data acquired from test pits. The information on granular deposits and associated geotechnical information acquired from the test pits was compiled into a single table in the Microsoft Excel dataset (Figure 5). However, when the spatial information was converted to ESRI shapefiles, the data were split into granular deposits and geotechnical test pits. The test pits were converted to a point file, whereas the granular deposits were converted to a set of point, line, and polygon features depending upon the number of points used to describe the location of the deposit. Due to software limitations the polygon features are depicted as closed lines. Descriptions of the database fields can be found in Appendix B Table B3.

TABLE 3

SUMMARY OF GRANULAR PROSPECTS

NTS 85F ZONE 11V SHEET 1 of 3

		GEOLOGIC LANDFORM								SURFACE TOPOGRAPHY					DEPOSIT SIZE			
PROSPECT	UTM GRID	Esker	Kame	Outwash	Ice-contact deposit	Terrace	Delta	Cone or fan	Talus	Ridge	Hill	Plain	Slope	Bench	Small	Medium	Large	COMMENTS
1	MT5878 MT6077 MT6276 MT6474												X			X		
2	MT5979 MT6178 MT6277												X			X		
2A	MT4786 MT4985 MT5184 MT5383 MT5681 MT5980 MT6381 MT6279 MT6476												X				X	Beach ridges
3	MT6081												X		X			

Figure 2. Example of granular deposit report data prepared by J. D. Mollard and Associates Ltd. (1993). Note, the coded values within the UTM grid field were truncated to reference the military grid reference system (MGRS).

	A	B	C	D	E	F	G	H
1	NTS_SHEET	PROSPECT	UTM_ZONE	EASTING	NORTHING	UTM GRID	TYPE	UID
74	85F	1	11V	458000	6878000	MT5878	POLYGON	85F1
75	85F	1	11V	460000	6877000	MT6077	POLYGON	85F1
76	85F	1	11V	462000	6876000	MT6276	POLYGON	85F1
77	85F	1	11V	464000	6874000	MT6474	POLYGON	85F1
78	85F	2	11V	459000	6879000	MT5979	POLYGON	85F2
79	85F	2	11V	461000	6878000	MT6178	POLYGON	85F2
80	85F	2	11V	462000	6877000	MT6277	POLYGON	85F2
81	85F	2A	11V	447000	6886000	MT4786	POLYGON	85F2A
82	85F	2A	11V	449000	6885000	MT4985	POLYGON	85F2A
83	85F	2A	11V	451000	6884000	MT5184	POLYGON	85F2A
84	85F	2A	11V	453000	6883000	MT5383	POLYGON	85F2A
85	85F	2A	11V	456000	6881000	MT5681	POLYGON	85F2A
86	85F	2A	11V	459000	6880000	MT5980	POLYGON	85F2A
87	85F	2A	11V	463000	6881000	MT6381	POLYGON	85F2A
88	85F	2A	11V	462000	6879000	MT6279	POLYGON	85F2A
89	85F	2A	11V	464000	6876000	MT6476	POLYGON	85F2A
90	85F	3	11V	460000	6881000	MT6081	POINT	85F3

Figure 3. Screenshot of the "Mollard" granular deposit database location table.

A	B	C	D	E	F	G	H	I	J	K	L
PROJ_NAME	CONTRACTOR	SPONSOR	UTM_ZONE	NTS_SHEET	PROSPECT	LANDFORM	TOPOGRAPHY	SIZE	COMMENT	SURF_GEO_INFERRED	UID
COMPILATION INVENTOI	J D MOLLARD AND ASSO	DIAND	11V	85F	1		SLOPE	MEDIUM	BEACH RIDGES	Lr	85F1
COMPILATION INVENTOI	J D MOLLARD AND ASSO	DIAND	11V	85F	2		SLOPE	MEDIUM	BEACH RIDGES	Lr	85F2
COMPILATION INVENTOI	J D MOLLARD AND ASSO	DIAND	11V	85F	3		SLOPE	SMALL	BEACH RIDGES	Lr	85F3
COMPILATION INVENTOI	J D MOLLARD AND ASSO	DIAND	11V	85F	4		SLOPE	MEDIUM	BEACH RIDGES	Lr	85F4
COMPILATION INVENTOI	J D MOLLARD AND ASSO	DIAND	11V	85F	5		SLOPE	MEDIUM	BEACH RIDGES	Lr	85F5
COMPILATION INVENTOI	J D MOLLARD AND ASSO	DIAND	11V	85F	6		SLOPE	SMALL	BEACH RIDGES	Lr	85F6
COMPILATION INVENTOI	J D MOLLARD AND ASSO	DIAND	11V	85F	7	TERACE	PLAIN	MEDIUM	BEACH RIDGES	Lr	85F7
COMPILATION INVENTOI	J D MOLLARD AND ASSO	DIAND	11V	85F	8		PLAIN	MEDIUM	STREAM BARS AND ABANDOND CHANNELS	U	85F8
COMPILATION INVENTOI	J D MOLLARD AND ASSO	DIAND	11V	85F	9		PLAIN	MEDIUM	STREAM BARS AND ABANDOND CHANNELS	U	85F9
COMPILATION INVENTOI	J D MOLLARD AND ASSO	DIAND	11V	85F	10		PLAIN	MEDIUM	STREAM BARS AND ABANDOND CHANNELS	U	85F10
COMPILATION INVENTOI	J D MOLLARD AND ASSO	DIAND	11V	85F	21		PLAIN	MEDIUM	STREAM BARS AND ABANDOND CHANNELS	U	85F21
COMPILATION INVENTOI	J D MOLLARD AND ASSO	DIAND	11V	85F	22		PLAIN	MEDIUM	STREAM BARS AND ABANDOND CHANNELS	U	85F22
COMPILATION INVENTOI	J D MOLLARD AND ASSO	DIAND	11V	85F	23		PLAIN	MEDIUM	STREAM BARS AND ABANDOND CHANNELS	U	85F23
COMPILATION INVENTOI	J D MOLLARD AND ASSO	DIAND	11V	85F	24		PLAIN	MEDIUM	STREAM BARS AND ABANDOND CHANNELS	U	85F24
COMPILATION INVENTOI	J D MOLLARD AND ASSO	DIAND	11V	85F	25		PLAIN	MEDIUM	STREAM BARS AND ABANDOND CHANNELS	U	85F25

Figure 4. Screenshot of the "Mollard" granular deposit database description table.

Granular Deposit	Landform	Estimated Volume (m3)	UTM Zone	Northing	Easting	Sample Number	Moisture Content (%)	USC	SPONSOR	CONTRACTOR	CO_JOB_NO	PROJ_NAME	SURF_GEO_INFERRED	DATE_SAMPLED	DATE_TESTED	SAMPLER	TESTER	SOIL_TYPE	DESCRIPT	%PASS_5MM_SIEVE	%PASS_0.08MM_SIEVE
1	Esker	50000	12	7282789	417490	13	1.1	SP	METALL MINI	EBA	0101-11159	IZOK PROJECT F	GFr	1993-07-14	1993-07-23	MAV	BL	SAND AND GRAVEL	TRACE SILT, O	50.7	0.4
2	Outwash	Limited	12	7283113	415211	12	2	SP	METALL MINI	EBA	0101-11159	IZOK PROJECT F	GF	1993-07-14	1993-07-23	MAV	BL	SAND	SOME GRAVEL	86.1	0.7
3	Esker	1,000,000 +	12	7285890	414628	10	6.3	GP	METALL MINI	EBA	0101-11159	IZOK PROJECT F	GFr	1993-07-13	1993-07-23	MAV	BL	GRAVEL AND SAND	TRACE SILT, O	42.4	2.6
3	Esker		12	7286153	413991	11	1.9	SP	METALL MINI	EBA	0101-11159	IZOK PROJECT F	GFr	1993-07-13	1993-07-13	MAV	BL	SAND AND GRAVEL	TRACE SILT, O	55.2	0.6
3	Esker		12	7286244	414909	9	2.2	SP	METALL MINI	EBA	0101-11159	IZOK PROJECT F	GFr	1993-07-13	1993-07-23	MAV	BL	SAND AND GRAVEL	TRACE SILT, O	57.7	1.2
3	Esker		12	7286957	412892	7	1.7	SP	METALL MINI	EBA	0101-11159	IZOK PROJECT F	GFr	1993-07-13	1993-07-22	MAV	BL	SAND	TRACE GRAVE	91.1	0.5
3	Esker		12	7287012	412911	8	2.1	SP	METALL MINI	EBA	0101-11159	IZOK PROJECT F	GFr	1993-07-13	1993-07-22	MAV	BL	SAND	GRAVELLY, TF	76.7	0.3
4	Esker	1,000,000 +	12	7286705	410893	40	2.2	SP	METALL MINI	EBA	0101-11159	IZOK PROJECT F	GFr	1993-07-16	1993-07-26	MAV	BL	SAND	TRACE GRAVE	99.5	0.8
4	Esker		12	7289462	407187	39	1.9	SP	METALL MINI	EBA	0101-11159	IZOK PROJECT F	GFr	1993-07-16	1993-07-26	MAV	BL	SAND	GRAVELLY, TF	65.4	0.8
4	Esker		12	7293527	403791	38	2.4	SP	METALL MINI	EBA	0101-11159	IZOK PROJECT F	GFr	1993-07-16	1993-07-26	MAV	BL	SAND	TRACE GRAVE	96	1.2
5	Esker/Kame	45000	12	7295545	402373	37	1.5	SP	METALL MINI	EBA	0101-11159	IZOK PROJECT F	GF	1993-07-16	1993-07-26	MAV	BL	SAND	TRACE GRAVE	94.8	1
6	Esker	60000	12	7298525	401344	36	3.5	SP	METALL MINI	EBA	0101-11159	IZOK PROJECT F	GFr	1993-07-16	1993-07-26	MAV	BL	SAND	GRAVELLY, TF	73.3	1.3
7	Outwash	Limited	12	7299800	403000								GF								
8	Esker	45000	12	7301945	401279	35	2.4	SP	METALL MINI	EBA	0101-11159	IZOK PROJECT F	GFr	1993-07-16	1993-07-26	MAV	BL	SAND	TRACE GRAVE	90	0.7
9	Outwash	Limited	12	7304400	402600								GF								
10	Outwash	Limited	12	7308500	402350								GF								
11	Outwash	Limited	12	7110100	402600								GF								
12	Outwash	100000	12	7313368	402366	34	1.9	SP	METALL MINI	EBA	0101-11159	IZOK PROJECT F	GF	1993-07-16	1993-07-26	MAV	BL	SAND AND GRAVEL	TRACE SILT. O	55.4	0.6
13	Esker	200000	12	7315204	399647	33	2.9	GP	METALL MINI	EBA	0101-11159	IZOK PROJECT F	GFr	1993-07-16	1993-07-26	MAV	BL	GRAVEL	SANDY. TRACI	36.2	3.5
14	Esker	300000	12	7317089	398561	32	4.1	SP	METALL MINI	EBA	0101-11159	IZOK PROJECT F	GFr	1993-07-16	1993-07-26	MAV	BL	SAND	TRACE GRAVE	99.4	3.5
15	Outwash	Limited	12	7315600	402400								GF								
16	Outwash	Limited	12	7320600	405000								GF								
17	Outwash	Limited	12	7321800	403400								GF								
18	Esker	1,000,000 +	12	7356774	387685	31	0.9	GP	METALL MINI	EBA	0101-11159	IZOK PROJECT F	GFr	1993-07-16	1993-07-26	MAV	BL	GRAVEL	SANDY. TRACI	35.2	0.3
19	Esker	1,00.0,000 +	12	7364315	391722	30	3.1	GW/GM	METALL MINI	EBA	0101-11159	IZOK PROJECT F	GFr	1993-07-16	1993-07-24	MAV	BL	GRAVEL AND SAND	TRACE SILT, O	44.8	6.4
19	Esker		12	7365392	389829	29	2.6	SP/SM	METALL MINI	EBA	0101-11159	IZOK PROJECT F	GFr	1993-07-16	1993-07-24	MAV	BL	SAND AND GRAVEL	TRACE SILT, O	57.6	5.4
19	Esker		12	7369583	385461	28	3.2	GP	METALL MINI	EBA	0101-11159	IZOK PROJECT F	GFr	1993-07-16	1993-07-24	MAV	BL	GRAVEL AND SAND	TRACE SILT, O	49.9	1.4
20	Esker	300000	12	7372858	382265	27	2.9	GP	METALL MINI	EBA	0101-11159	IZOK PROJECT F	GFr	1993-07-16	1993-07-24	MAV	BL	GRAVEL AND SAND	TRACE SILT, O	43.2	1.6
20	Esker		12	7376832	382653	26	1.9	SW	METALL MINI	EBA	0101-11159	IZOK PROJECT F	GFr	1993-07-16	1993-07-24	MAV	BL	SAND AND GRAVEL	TRACE SILT, O	56.9	3.1
21	Esker	20	12	7380300	380500								GFr								
22	Esker	40000	12	7390795	380287	25	3.7	SP	METALL MINI	EBA	0101-11159	IZOK PROJECT F	GFr	1993-07-16	1993-07-24	MAV	BL	SAND AND GRAVEL	TRACE SILT, O	51.2	3.6
23	Esker	Limited	12	7391800	377000								GFr								
24	Esker	120000	12	7395260	377116	24	1.5	GP	METALL MINI	EBA	0101-11159	IZOK PROJECT F	GFr	1993-07-15	1993-07-24	MAV	BL	GRAVEL AND SAND	TRACE SILT, O	43	1.3
25	Esker	50000	12	7401601	376247	23	4.6	SP	METALL MINI	EBA	0101-11159	IZOK PROJECT F	GFr	1993-07-15	1993-07-24	MAV	BL	SAND	TRACE GRAVE	93.7	3.3
26	Esker	35000	12	7409600	371700								GFr								
27	Esker	400000	12	7410673	372332	22	2.3	SP	METALL MINI	EBA	0101-11159	IZOK PROJECT F	GFr	1993-07-15	1993-07-24	MAV	BL	SAND AND GRAVEL	TRACE SILT, O	64.3	1.9
27	Esker		12	7415622	370732	21	3.4	SP	METALL MINI	EBA	0101-11159	IZOK PROJECT F	GFr	1993-07-15	1993-07-24	MAV	BL	SAND	TRACE GRAVE	92.6	0.8
28	Outwash	200000	11	7424220	628880	20	3.1	SP	METALL MINI	EBA	0101-11159	IZOK PROJECT F	GF	1993-07-15	1993-07-24	MAV	BL	SAND AND GRAVEL	TRACE SILT, O	58.4	1.6
29	Esker	Limited	11	7425450	629000								GFr								
30	Esker	Limited	11	7428500	627000								GFr								
31	Esker	75000	11	7430529	626217	19	2	SP	METALL MINI	EBA	0101-11159	IZOK PROJECT F	GFr	1993-07-15	1993-07-23	MAV	BL	SAND AND GRAVEL	TRACE SILT, O	52.8	1.5
32	Esker	30000	11	7434000	625000								GFr								
33	Esker	400000	11	7439668	622320	18							GFr	1993-07-15	1993-07-23	MAV	BL	SAND	TRACE SILT, O	100	6.2
34	Esker	Limited	11	7441400	621600		4	SP/SM	METALL MINI	EBA	0101-11159	IZOK PROJECT F	GFr								
35	Esker	Limited	11	7443100	621000								GFr								
36	Esker	25000	11	7444978	620462	17	1.5	GP	METALL MINI	EBA	0101-11159	IZOK PROJECT F	GFr	1993-07-15	1993-07-23	MAV	BL	GRAVEL	SOME SAND, T	13.7	1.5
37	Esker	75000	11	7448848	619478	16	4.1	SP/SM	METALL MINI	EBA	0101-11159	IZOK PROJECT F	GFr	1993-07-15	1993-07-23	MAV	BL	SAND	TRACE GRAVE	99.4	8.1
38	Outwash	60000	11	7464685	612418	15	1.6	GW	METALL MINI	EBA	0101-11159	IZOK PROJECT F	GF	1993-07-15	1993-07-23	MAV	BL	GRAVEL AND SAND	TRACE SILT, O	47.2	1.2
39	Esker	100000	11	7470985	611676	8	1.6	SP	METALL MINI	EBA	0101-11159	IZOK PROJECT F	GFr	1993-07-13	1993-07-22	MAV	BL	SAND	GRAVELLY, TF	76.7	0.3
40	Esker	Limited	11	7474000	610150								GFr								
41	Outwash	Limited	11	7485000	606000								GF								

Figure 5. Screen shot of the “EBA” granular deposit database.

3.1.4 Supplementary Data for Analysis

Digitized versions of the surficial geology maps covering NTS sheets 75-M; 76-D, E, L, M; 85-I, J, P; and 86-A, H, I, P (Geological Survey of Canada, 2017a, 2017b, 2016a, 2016b, 2015, 2014a, 2014b; Kerr, 2018, 2014; Olthof et al., 2014; Stevens et al., 2017) were used to generate attributes for the geomorphic features and for analysis of the datasets (Figure 1). Digitized versions of the Permafrost Map of Canada (Heginbottom et al., 1995) and the Physiographic Region Map of Canada (Bostock, 2014) were also used in the GIS to generate attributes for digitized geomorphic features. The 1:50,000 scale CanVec waterbodies layer was used to identify boreholes that had been drilled into lake or pond beds (Natural Resources Canada, 2021).

3.2 Image Processing

The methods of Sladen et al. (2021) for pan-sharpening and orthorectifying the raw satellite imagery were improved upon and streamlined to reduce processing time from weeks to days. This involved automating the image processing using functions in both the ArcGIS Pro™ and PCI Geomatica® Banff libraries to produce orthorectified pansharpened imagery from the raw data in a batch. Although the imagery processed prior to March 2020 was converted to 3D following the same methods described in Sladen et al. (2021), imagery processed after March 2020 was not converted because the relative relief is very low.

3.3 Geomorphic Feature Digitization and Quality Control

Two adaptations were made to the feature digitization procedure outlined by Sladen et al. (2021). First, the features were identified and digitized at the 1:5,000 scale instead of the 1:10,000 scale used in Sladen et al. (2021), because the surface expression of ice wedge polygon networks in the mapping region are far less pronounced than in the western Arctic, and therefore most ice wedge polygon features were not identifiable at the smaller scale. Since access to a 3D workstation was limited, therefore feature digitization was conducted using some 3D imagery with Summit as well as 2D imagery with ArcGIS Pro. Both the 3D and 2D digitization procedures followed the process outlined in Sladen et al. (2021) with the major exception that digitization in the 2D procedure occurred in ArcGIS Pro. This modification to the procedure was deemed acceptable due to the low relief of the Canadian Shield region.

3.3.1 Classification

Feature classification also follows Sladen et al. (2021) (Appendix C), with features broadly classified as periglacial, hydrological, or mass wasting, and within each of these categories are a set of landforms that are mapped. However, two feature types were added to the periglacial class as they were not observed by Sladen et al. (2021): creep of frozen ground and permafrost peatland. The classification scheme for the two feature types is described below. The larger scale used in this study also allowed for small peatlands to be mapped. In the Slave region, the peatlands are generally not expansive, and those at more northerly locations often expressed ice wedges at their surface whereas peatlands at more southerly locations often do not, as was also the case within the Dempster and Inuvik-Tuktoyaktuk corridor (Sladen et al. 2021).

3.3.1.1 Creep of Frozen Ground

The landform resembles lateral spread mass wasting, but rather than slope failure along a sheer plain, the distortion of the ground is attributed to gradual creep (or time-dependent deformation) of ice-rich ground at depth (Dredge et al., 1999; Wolfe et al., 2017) (Figure 6). If creep occurs beneath an ice-wedge polygon network, the network becomes laterally extended, and troughs between the polygons are relatively deeply incised, giving the appearance that the polygon surface pattern is being stretched apart (Figure 6b). The ice-wedge polygons are often the high-centre sub-type (Mackay, 2000). The plastic deformation of ice-rich ground at depth may itself induce little or no overall volume change and can occur at temperatures well below freezing (Associate Committee on Geotechnical Research, 1988). However, there may also be some evidence of thermokarst processes, in addition to creep, associated with melt of wedge ice (formation of deep troughs between high-centred polygons) or other ground ice at depth (kettle lake formation). The lateral extension can occur on very gentle slopes or otherwise flat terrain. The digitizing criteria applicable to landforms related to creep are outlined in Table 1.

3.3.1.2 Permafrost Peatland

Peatland features are characterized as flat areas of well-drained peat that developed due to the accumulation of organic material and characteristically have a ground cover of light-coloured reindeer lichen (*Cladonia rangiferina*) (Gibson et al., 2020) (Figure 7a). However, peatlands may burn over during a forest fire event, which removes the reindeer lichen and exposes the underlying dark-hued organic soil, and it may take decades for the reindeer moss to return (Figure 7b). Ice-wedge polygon networks and or thermokarst depressions may be present within these peatlands, with the depressions typically formed as circular or elliptical collapse scars, and below treeline black spruce (*Picea mariana*) may form a canopy, but this canopy may be sparse or absent (Gibson et al., 2020; Zoltai, 1993; Zoltai and Tarnocai, 1975). Peatlands are in a state of dynamic equilibrium constantly undergoing a ~600-year cycle of permafrost aggradation, degradation, and re-aggradation (Gibson et al., 2020; Zoltai, 1993). During this cycle the elevation of the peatland relative to the surrounding area changes significantly with respect to the local water table, increasing during aggradation phases and decreasing during degradation phases (Gibson et al., 2020; Zoltai, 1993). Due to the dynamic nature of these features they have a wide variety of appearances in imagery (Gibson et al., 2020). Table 2 shows the mapping criteria used for identifying these features.

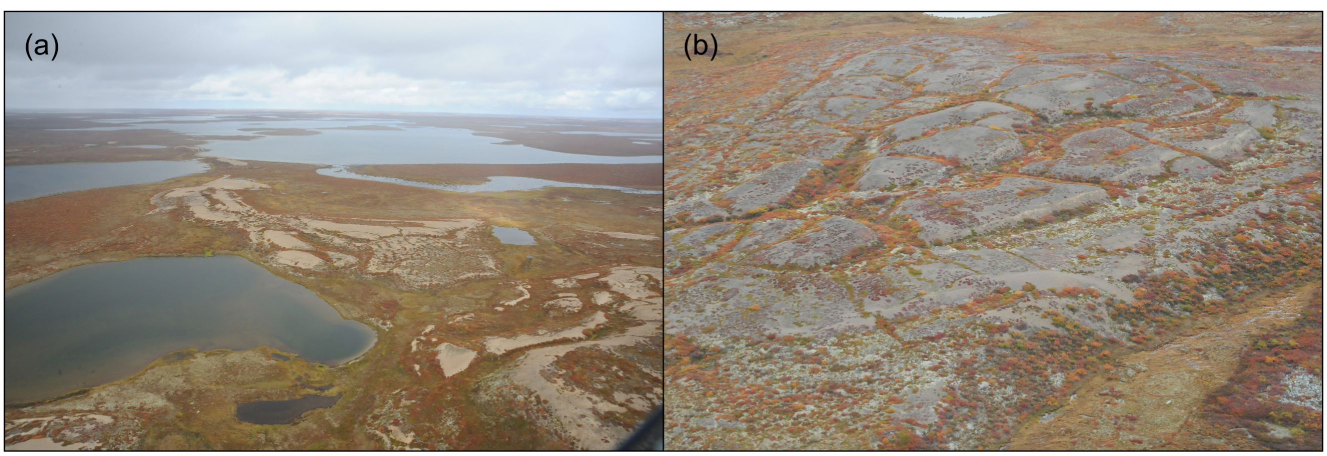

Figure 6: Examples of creep of frozen ground in the Slave Geological Province. (a) Photograph by P.D. Morse (64°43’33.4” North, 110°06’53.2” West; NRCan photo 2021-709. (b) Photograph by P.D. Morse (64°35’40.3” North, 110°11’07.8” West; NRCan photo 2021-710).

Table 2. Mapping criteria for creep of frozen ground and permafrost peatland periglacial features.

Feature type	Subtype	Criteria

Creep of frozen ground	N/A	• Commonly associated with glaciofluvial deposits
		• Resembles lateral spread mass wasting, but no failure has occurred
		• Kettle lakes (thermokarst) often present
		• If ice-wedge polygons are present
		  ○ Surface pattern is distorted by lateral extension or compression
		  ○ Polygons are often high-centred and separated by deep troughs (thermokarst) that may exhibit ponding

Peatland	Polygonal
	N/A
		• Present in flat low-lying areas
		• Uniform light-coloured vegetation mat with mottled patches, often distinctly different to surrounding vegetation cover
		  ○ Vegetation (with or without trees) is often lighter-coloured compared to surroundings when below treeline
		  ○ Vegetation mat may be darker-coloured compared to surroundings when the peatland has been burned in the past
		• Streams or discontinuous thaw scars (may be ponded or a lawn) within the feature
		• Can be evidence of ice-wedge polygon features
		  ○ Indicated in subtype field
		• Absence or sparse distribution of trees when features are below treeline

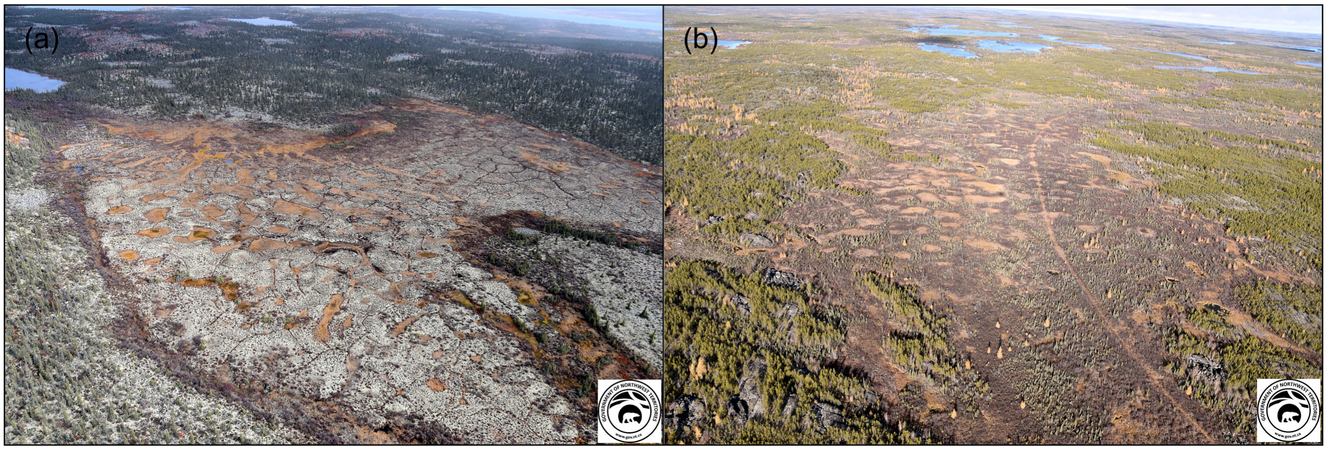

Figure 7: Examples of permafrost peatland in the Slave Geological Province. (a) Unburned since at least 1950 (63°26’59.8” North, 112°02’34.2” West, photograph courtesy of Northwest Territories Geological Survey). (b) Burned in 1996 (63°01’53.3” North, 113°28’10.5” West, photograph courtesy of Northwest Territories Geological Survey).

3.3.2 Quality Control

Quality control was conducted in a method similar to Sladen et al. (2021). A 2 km by 2 km grid of the entire mapping region was generated, and every grid cell that contained a digitized feature or was bordered by a cell that contained a digitized feature was checked by an experienced mapping reviewer. The reviewer systematically inspected the imagery for the entire mapping region and ensured that they agreed with what was mapped and that no features were missed by the primary mapper. Any discrepancies were noted in the comment attribute of a feature, and any missed features were digitized. These changes were reviewed with the primary mapper to ensure agreement and were then implemented. Approximately 50% of the grid cells either contained a digitized feature or bordered a cell that contained a feature. To determine if any features had been missed in the initial mapping, 40% of the remaining grid cells without a feature or not adjacent to a cell with a feature (20% of total) were randomly selected and checked by the reviewer. In total, 70% of all grid cells in the entire mapping region were reviewed during quality control, and only 9 new features were added from the randomly selected cells. This strategy saved time while ensuring that all features were checked by the reviewer and providing sufficient assurance that likely very few features were missed. The final data layers were inspected in ArcGIS Pro by the primary mapper to ensure that no inconsistencies such as missing points, missing attribute data, or non-closed shapes were present.

3.4 Geomorphic Feature Analysis

Feature attributes including surficial geology are assigned to each geomorphic feature according to the feature's centroid using a series of Python scripts (Sladen et al., 2021) (Appendix D). Descriptions of the geomorphic feature database fields can be found in Appendix B Tables B4 to B7. In preliminary analyses of the digitized feature dataset, we identified a bias related to the surficial geology attribute and the use of vectors, such that the area analysis calculations of feature coverage according to surficial geology attribute data are biased toward the location of the centroid. For example, if the centroid of an extensive ice-wedge polygon feature fell on a smaller glaciofluvial esker, the surficial geology unit would result in an ice-wedge polygon area entirely attributed as glaciofluvial esker, even though the esker may only make up a smaller area than the ice-wedge polygon area. To rectify this, a raster-based analysis approach was used to calculate the percentage of each surficial geology unit covered by each feature, and to determine the percentage of each feature type that is in each surficial geology unit. First, surficial geology datasets were rasterized to a pixel size of 2 m, and the pixel information within the mapping region was summarized and used to calculate total area of each surficial geology unit. The pixels within the extents of feature type polygons were then extracted.

The geomorphic feature database was also compared against the permafrost related geomorphic feature points included as a part of the surficial geology (Geological Survey of Canada, 2017a, 2017b, 2016a, 2016b, 2015, 2014a, 2014b; Kerr, 2018, 2014; Olthof et al., 2014; Stevens et al., 2017 Wolfe et al., 2017). Geomorphic feature points were identified as permafrost related based on their feature type attribute. The following feature types were extracted: gelifluction-lobe or solifluction-lobe, debris-flow track, landslide scar, retrogressive thaw flow, unspecified slope-movement, ice-contact delta, palsa or lithalsa, patterned ground, pingo, rock glacier, rock pingo, and thermokarst depression. This dataset was then subset to only include points within the mapping area. A series of spatial comparisons identified where the same features were mapped in each dataset by first looking for exact overlap between the datasets and then by expanding the search criteria to identify features that were within 250 m of each other to account the potential of mapping discrepancies and/or registration error of the datasets.

3.5 Geotechnical Borehole Analysis

The positional information of each borehole was used to generate an initial spatial dataset. Our analysis zone was comprised of the NTS sheets compiled to cover the corridor mapping extent and projected to UTM zone 12 which was the projection used for mapping. A borehole analysis subset was created from the boreholes within this analysis zone. Spatial analysis was used to assign a surficial geology unit to each location in the subset. This allowed the borehole information to be aggregated by surficial geology unit for analysis and to relate the borehole information to the digitized features that fall within the same surficial unit. The thickness of surficial material was determined for each borehole that reached bedrock.

The surficial geology unit into which each borehole was drilled was assigned to the spatial data based on inference from the soil type description at a depth of 0.5 m, except where very shallow boreholes terminated at a lesser depth, in which case the deepest borehole sample was used. Surficial geology assigned to the spatial data was inferred based on a hierarchy of the soil type descriptions and comments in the borehole database according to the scheme shown in Table 3. Using the depth to bedrock information, boreholes drilled in glacial sediments were then split further into veneer, blanket, and undifferentiated subclasses. Following the V2.3.14 of the GSC surficial data model (Deblonde et al., 2018), boreholes with depth to bedrock less than or equal to 2 m were classed as veneer, greater than 2 m were classed as blanket, and boreholes with no depth to bedrock information were classed as undifferentiated. These results were then manually validated against ESRI base map high resolution imagery with any questionable classifications resulting in a revaluation of the classification hierarchy. One borehole (11157-18A) only contained records deeper than 0.5 m, so its surficial geology was classified as undifferentiated.

Table 3: Inferred surficial geology unit based on the soil description at 0.5 m depth.

Hierarchy level	Soil type substring	Inferred surficial geology unit code
1	till	T
2	organic	O
3	silt + notes describing soil	L
4	sand	GF
5	silt	GF
6	no recovery	U
7	loss	U
8	rock	R
9	boulder	T
10	cobble	T
11	gran	R
12	tuff	R
13	gabbro	R
14	wacke	R
15	volcan	R
16	pegmatite	R
17	colluvium	R
18	andesite	R
19	gravel	GF
20	peat	O
21	surface	U
22	overburden	U
23	nan (not a number)	U
24	clay	M
25	ice	GF
26	sediment	U

Note: See Figure 1 for surficial geology unit legend, except for M which represents marine sediments: undifferentiated.

3.6 Granular Deposit Analysis

Apart from the geotechnical data from the test pit samples (EBA Engineering Consultants Ltd. 1993a), the granular deposit databases provided little information of value to this work due to a general lack of spatial information for most of the records. Additionally, for records with spatial data, the reported line and polygon features were not developed with any spatial precision. Therefore only the point features within the granular deposit databases were assessed as they could be easily analyzed spatially and provide a representative sample of the information contained within the granular deposit databases.

First, the granular deposit point data was subset to the analysis zone (i.e. granular analysis subset) described in the previous section. Next, surficial geology was inferred based on a hierarchy of the landform descriptions and comments in the database according to the scheme in Table 4. As with the geotechnical borehole database, a hierarchical substring search was used to infer surficial geology. First, we searched for landform descriptions identical to known surficial geology subclasses (*e.g.*, esker, kame, etc.); then, the landform descriptions which comprised known surficial geology subclasses as a part of the text (*e.g.*, "esker, delta"); and finally, the comments were searched for entries containing the word "beach". Any feature that did not satisfy any of the above conditions was classified as undifferentiated sediments. The geotechnical information from the test pit samples was summarized according to surficial geology unit, and the respective landform information was used to create a matrix of landforms with respect to surficial geology units.

Table 4: Inferred surficial geology based on landform or comment descriptions.

Hierarchy level	Landform or comment substring	Inferred surficial geology code
1	ESKER	GFr
1	KAME	GFk
1	ICE-CONTACT DEPOSIT	GFc
1	OUTWASH	GF
2	*ESKER*	GF
2	*KAME*	GF
2	*ICE-CONTACT DEPOSIT*	GF
2	*OUTWASH*	GF
3	*BEACH*	Lr

Note: The * denotes where the search allows other text to be present. Lr represents lacustrine sediments: beach. GFk represents glaciofluvial sediments: kame terrace. See Figure 1 for surficial geology unit legend.

4 Results

4.1 Geomorphic Features

Using the satellite imagery, a total of 1393 geomorphic features (9732 ha), comprised by 10 different feature types, were identified and digitized (Figure 8). In count and total area, periglacial class features are by far the most common (n = 1291) and extensive (8923.07 ha), followed distantly by hydrological class features (n = 88; 790.67 ha) and mass movement class features (n = 14; 18.61 ha) (Table 5). About 70% of all features are ice wedge polygons, and another 15% are peatlands. About 58% of the area of the features is due to ice wedge polygons, but despite their relatively low count (n = 65) areas affected by creep of frozen ground make up about 17% of the total feature area, whereas more numerous peatlands comprise less total area at about 13%.

Surficial geology has a substantial influence on the distribution of features (Figure 9 to 11). For example, marine and littoral near shore sediments (Mn) have expansive ice-wedge polygon networks, which account for nearly 100% of the area of mapped landforms within this surficial geology unit, and though they are relatively few in number (Figure 9), the mapped features cover approximately 45% of the extent of Mn sediments (Figure 10). Eolian sediments also have relatively few features (n = 3), but these cover just over 40% of this unit's area, predominately due to creep of frozen ground (Figure 10). In contrast, the combined glacial sediments (Th, Tm, Tr, Tv, Tb and T) are the most extensive in the mapping area (Figure 11), and feature counts and areas are high (Figure 9 and Figure 11). However, feature density is very low and less than 1% of each unit is covered by digitized features (Figure 10). The influence of the extent of surficial deposits on feature distribution is evidenced by Figure 9 and Figure 11 where the surficial geology units with the five highest feature counts are among the six most extensive surficial geology units. There is also a bias with respect to bedrock (R), because the features we mapped can be smaller than the minimum polygon size used for surficial geology mapping, hence the attribution to rock (R) is common as this unit is extensive in the region but small deposits of other surficial materials are commonplace and permit features such as peatlands or ice-wedge polygons to form in local depressions.

For periglacial features, almost 87% of creep of frozen ground area occurs within glaciofluvial surficial geology classes (GF, GFp, GFc, and GFr) (Figure 12a). Approximately 30% of the peatland feature area occurs on organic deposits, but just over 51% is associated with glacial sediments (Th, Tv, and Tb) (Figure 12b). The ice-wedge polygon is the most diverse feature, and is associated with 21 of the 25 surficial geology units that have mapped features, but approximately 59% of the area covered by the ice-wedge polygon features is within four surficial geology units (O, Mn, Tb, Tv) (Figure 12c).

Approximately 29% of the string/net fen feature area is associated with organic deposits, but another 20% of the area is related to glacial blanket sediments and 14% to glaciolacustrine undifferentiated sediments (Figure 12d).

For hydrological features, about 35% of beaded stream area is associated with marine blanket sediments, where ice-wedge polygons are the dominant periglacial feature, though another 45% of beaded streams are associated with the top three highest areal extents of ice wedge polygons (O, Tb, Tv) (Figure 9 and Figure 13a). Only two drained-lake basin features were mapped, and approximately 46% of the area that they covered was underlain by glacial sediments (Th, Tv, and Tb) with the remaining area being underlain by organic deposits and bedrock (Figure 13b). Icings and the snowpack surficial geology unit (Isn) are closely related, with about 32% of icing area covering just over 70% Isn area (Figure 10 and Figure 13c). However, another 38% of icing area is distributed equally between alluvium and bedrock with the remaining icing area distributed over 12 other surficial geology units (Ap, At, Mb, GMd, GLd, GL, GFc, GFr, GF, Tv, Tb, U) (Figure 13c). Of the 14 thermokarst lake/pond features, nearly 41% of their area is associated with glaciofluvial esker sediments, about 29% is associated with organic deposits, with the remainder distributed over another 7 surficial geology units (Mb, GMd, GFp, Th, Tv, Tb, R) (Figure 13d).

Of the comparatively small set of mass movement features, two solifluction features are predominantly (65%) related to glaciofluvial esker (Figure 14a). The unclassified mass movement features occur exclusively in the northern-most region of the mapping area on riverbanks, and approximately 59% of their area is underlain by marine sediments (Mn and Mb) with the remaining area underlain by alluvial sediments (Figure 9 and Figure 14b)

One hundred thirty-nine permafrost related geomorphic feature points were extracted from the surficial geology datasets (Geological Survey of Canada, 2017a, 2017b, 2016a, 2016b, 2015, 2014a, 2014b; Kerr, 2018, 2014; Olthof et al., 2014; Stevens et al., 2017)). This included 120 patterned ground features broken down into 47 ice-wedge polygon features and 73 unspecified features. It also included 16 thermokarst depressions and 3 gelifluction/solifluction features. The extracted points were compared to all geomorphic features mapped in this work (Figure 8). However, the comparison only produced meaningful results for ice-wedge polygon, peatland, and creep of frozen ground features. This was because several points were either too far away from any mapped feature, or the feature type represented by the point and the mapped polygon did not match. The comparison showed that significantly more features were identified in our analysis and there is some agreement between the datasets (Table 6). However, the mapping criteria used to generate the two datasets are different. For example, the patterned ground geomorphic feature point type includes not only ice-wedge polygons but also any other form of patterned ground such as hummocky terrain visible in 1:2000 scale aerial photos used to generate the surficial geology maps.

Table 5. Geomorphic feature counts and areas.

Feature class	Feature type	Count	Area (ha)
Periglacial	Creep of frozen ground	65	1645.15
	Ice wedge polygon	974	5638.82
	String/ net fen	46	342.09
	Peatland	206	1297.02
	Total	1291	8923.07
Hydrological	Beaded stream	52	115.26
	Lake / pond affected by thermokarst	14	72.40
	Drained-lake basin	2	27.74
	Icing	20	575.27
	Total	88	790.67
Mass movement	Unclassified	12	16.04
	Solifluction	2	2.57
	Total	14	18.61

Table 6: Geomorphic feature – surficial geology feature point comparison results

Geomorphic features	Number of geomorphic features	Number of surficial geology feature points intersecting geomorphic features	Number of surficial geology feature points within 250 m of geomorphic features
Ice-wedge polygon	974	31 Total 2 Thermokarst depression 29 Patterned ground 7 Ice-wedge polygon 22 Unspecified	56 Total 6 Thermokarst depression 50 Patterned ground 19 Ice-wedge polygon 31 Unspecified
Peatland	206	3 Ice-wedge polygon	2 Thermokarst depression 3 Ice-wedge polygon
Peatland - Polygonal	27	1 Ice-wedge polygon	1 Thermokarst depression 1 Ice-wedge polygon
Creep of frozen ground	65	18 Patterned ground - Unspecified	21 Patterned ground - Unspecified
Ice-wedge polygon, peatland, creep of frozen ground	1245	52 Total 2 Thermokarst depression 50 Patterned ground 10 Ice-wedge polygon 40 Unspecified	73 Total 7 Thermokarst depression 66 Patterned ground 21 Ice-wedge polygon 45 Unspecified

Note: The final row reflects that some surficial geology points satisfied multiple selection conditions. For example, five patterned ground features were within 250 meters of mapped IWP and COFG features.

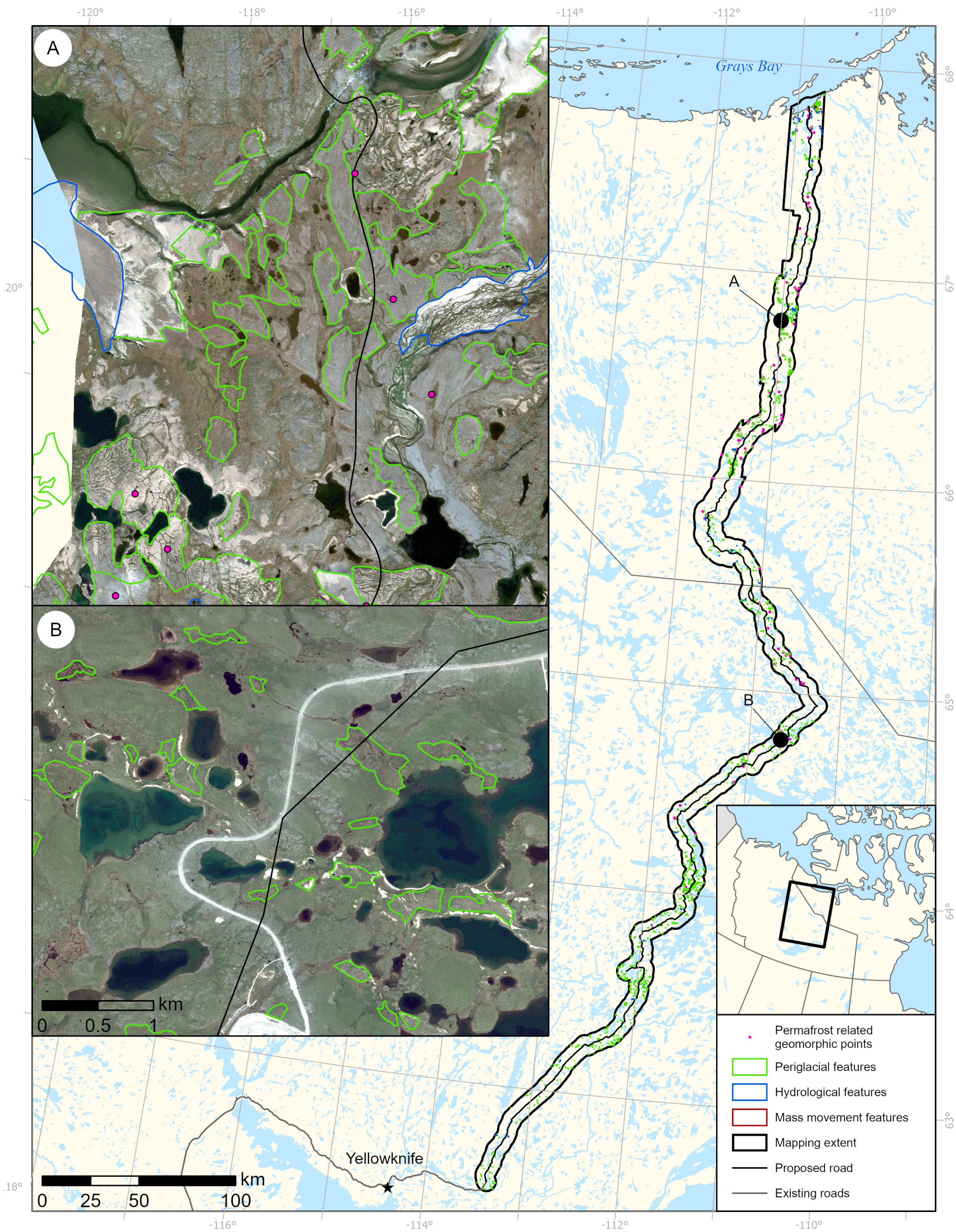

Figure 8. Mapped geomorphic features and permafrost related geomorphic feature points extracted from surficial geology maps (Geological Survey of Canada, 2017a, 2017b, 2016a, 2016b, 2015, 2014a, 2014b; Kerr, 2018, 2014; Olthof et al., 2014; Stevens et al., 2017), with more detailed examples shown in insets A and B. Inset A shows the proposed road centre line crossing a number of periglacial features that include creep of frozen ground, and inset B shows mapped features in the vicinity of the Ekati Diamond Mine.

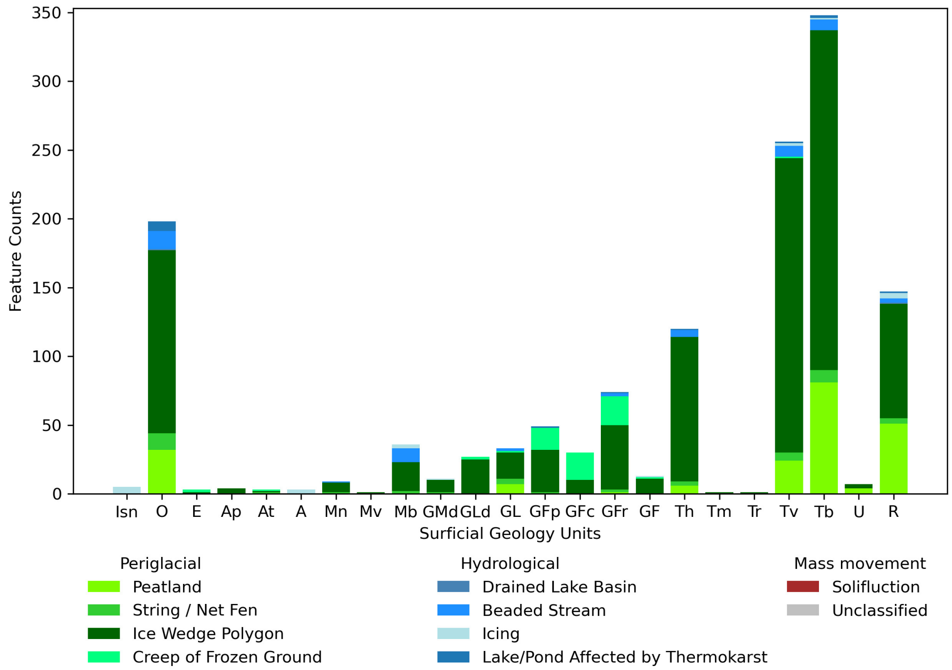

Figure 9. Feature counts according to surficial geology unit. The feature types are shown as shades of green for periglacial features and blue for hydrological features. See Figure 1 for surficial geology unit legend. Note: The figure is generated using the attribute data, which assigns the surficial geology unit according to the centroid of the polygon, but we recognize that some features cover more than one unit.

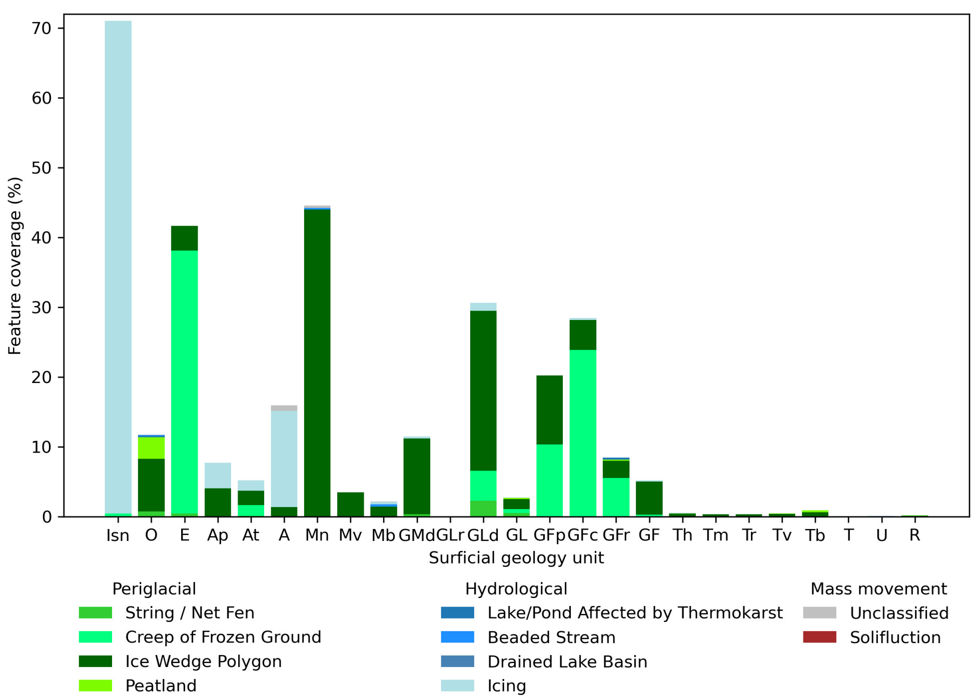

Figure 10. Percent area of surficial geology unit that is mapped with features. The feature types are shown as shades of green for periglacial features and blue for hydrological features. See Figure 1 for surficial geology unit legend.

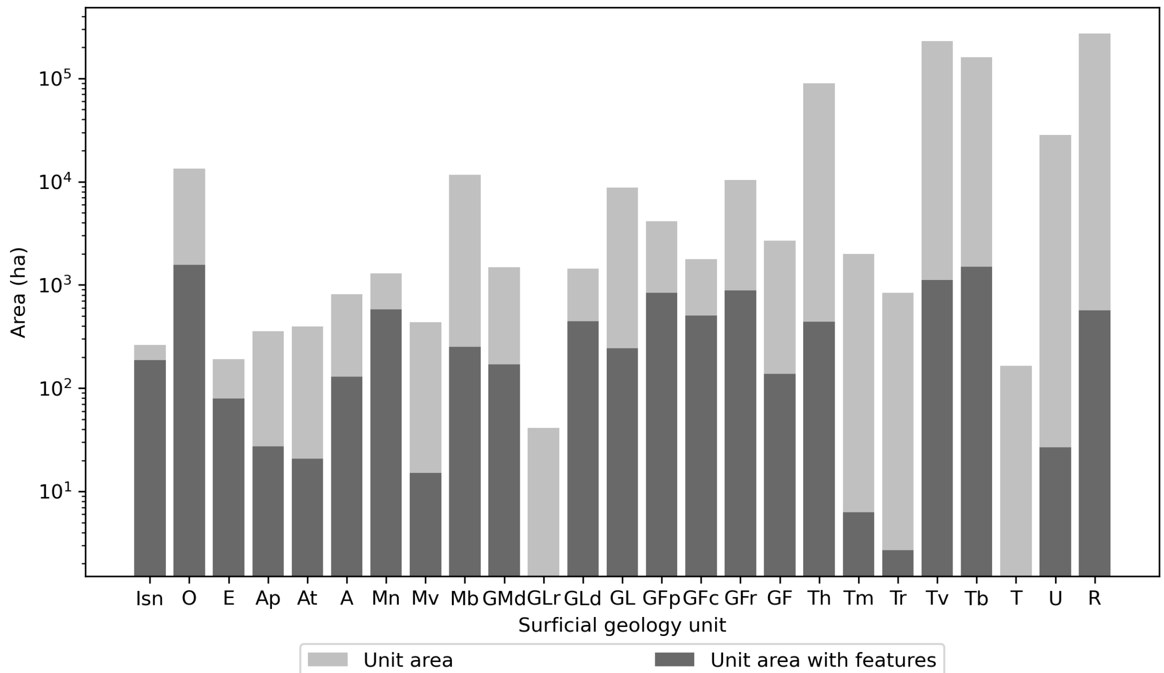

Figure 11. Total feature area and total unit area according to surficial geology. Note the log scale of the y-axis.

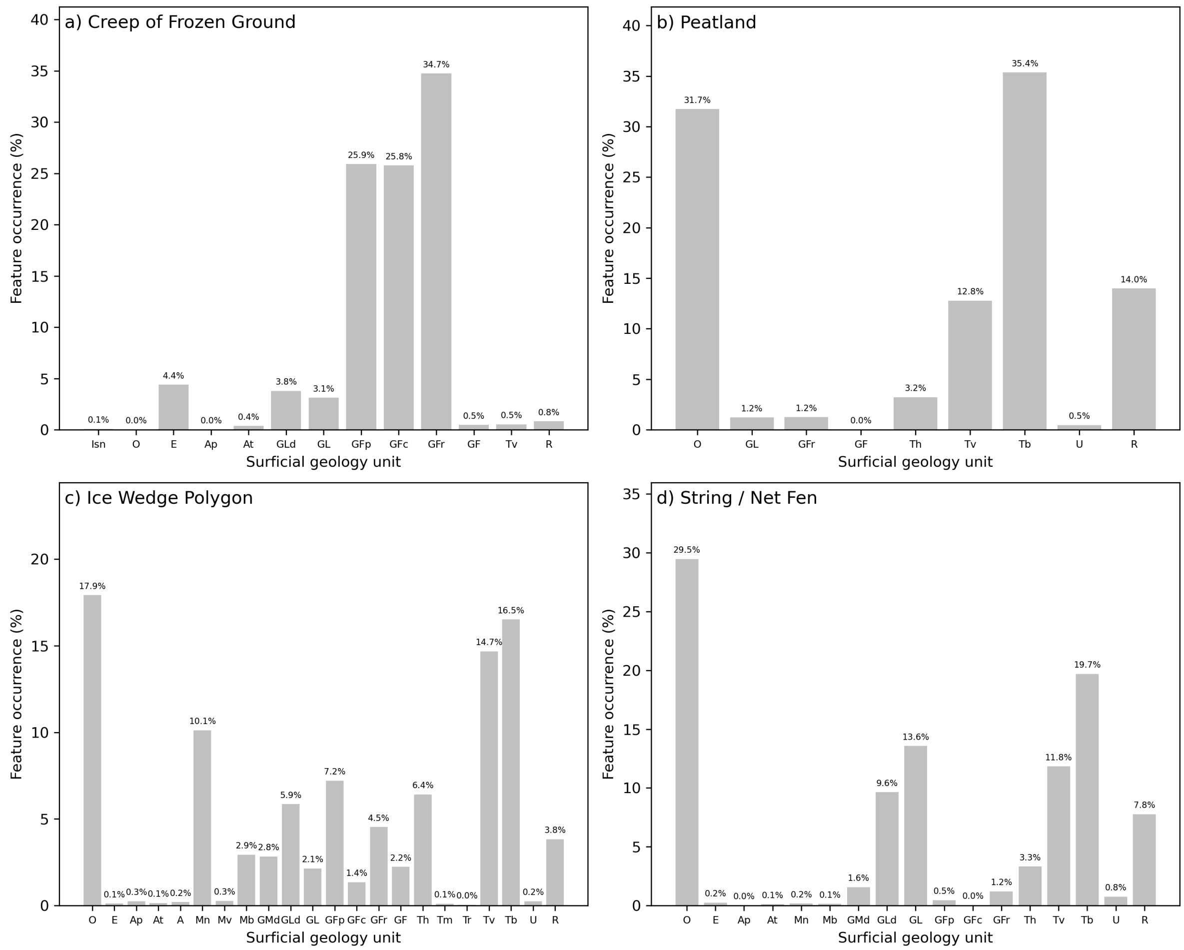

Figure 12. Distributions of periglacial feature area according to surficial geology. Feature types are ordered as: a) creep of frozen ground; b) peatland; c) ice wedge polygon; and d) string/net fen.

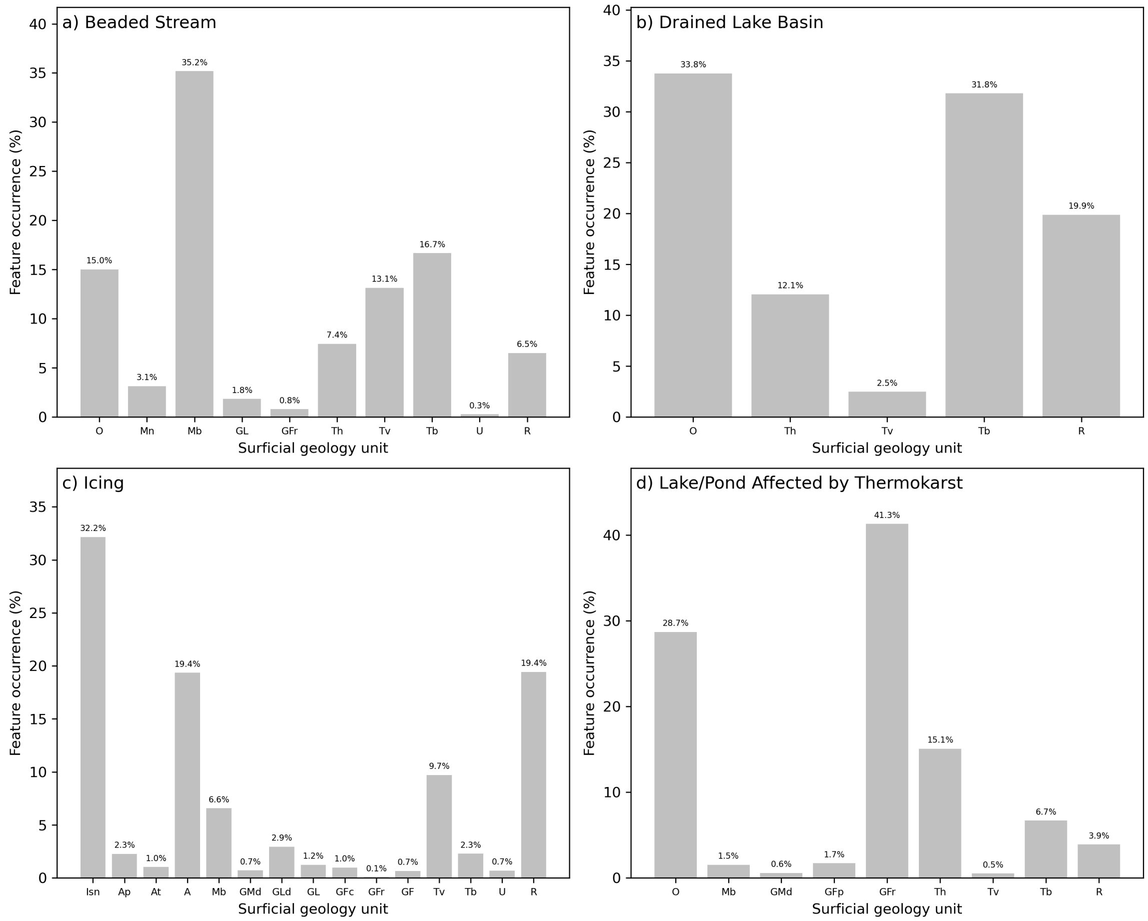

Figure 13. Distributions of hydrological feature area according to surficial geology. Feature types are ordered as: a) beaded stream; b) drained-lake basin; c) icing; d) lake/pond affected by thermokarst.

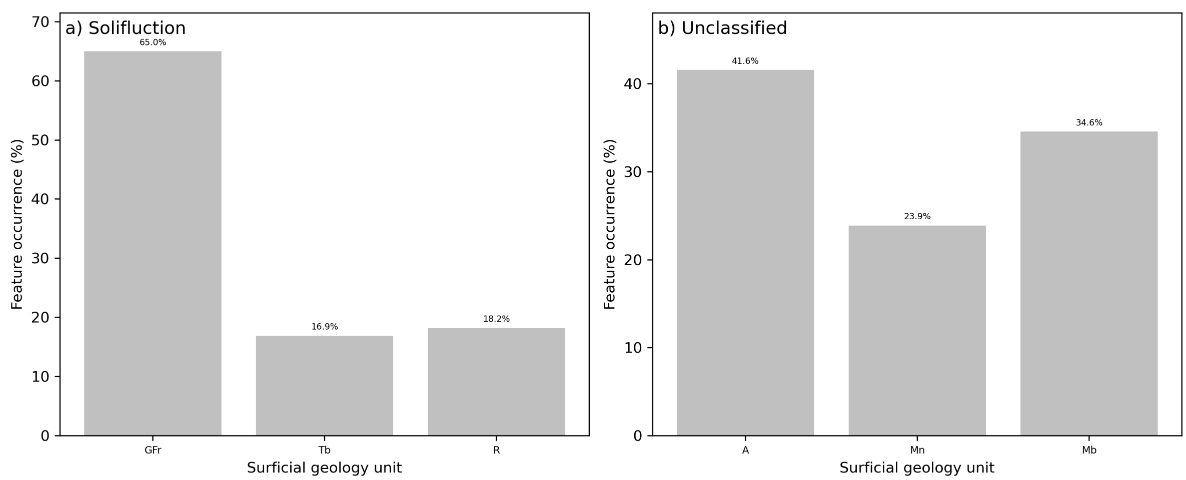

Figure 14. Distributions of mass movement feature area according to surficial geology. Feature types are ordered as: a) solifluction; and b) unclassified mass movement. Surficial geology class

4.2 Geotechnical Boreholes

Data were compiled from 254 boreholes drilled within and surrounding the mapping area. A subset of 213 boreholes within the analysis zone were analyzed with respect to the surficial geology inferred from the set of digitized surficial geology maps (Figure 15). Boreholes were drilled for a variety of purposes and the level of detail recorded varied according to the needs of the originator. Of the subset boreholes, 34% were in undifferentiated glaciofluvial sediments, 33% were in glacial sediments (till), 14% were in bedrock, and 11% were in undifferentiated lacustrine sediments, with the remaining 8% in organic, marine and undifferentiated sediment units (Figure 16). Three of the boreholes were drilled at landforms that were mapped as a part of this research activity.

Ground ice content is recorded for 53 of the analysis subset boreholes. The largest number of ground ice records (21) were recorded in till blanket deposits, though ground ice is relatively common in undifferentiated glaciofluvial sediments and bedrock (Figure 16). Small surficial deposits are filtered out from the surficial geology data during map production, so as with other analysis with respect to the surficial geology, it is likely that ground ice associated with bedrock actually occurs in a different surficial geology unit.

Depth to bedrock was extracted from 172 boreholes with the largest number of records (51) being in till blanket deposits (Figure 17). Overall, overburden thicknesses ranged up to about 25.5 m and were greatest in glaciofluvial, till blanket, and marine deposits, with median thicknesses of about 8 m, 5.5 m, and 12 m, respectively. Figure 18 to 25 show the visible ground ice contents recorded for each borehole organized by surficial geology, and depth to bedrock is shown where available. Reported ground ice contents are typically between 10% and 30% visible ice but are up to 55% in undifferentiated glaciofluvial and 60% in glacial blanket sediment surficial geology units. A few borehole records showed visible ground ice was observed deeper than the calculated depth to bedrock (e.g. Figure 18). In these cases, the ice likely occupies cracks or fractures in the rock. For illustrative purposes, Figure 26 to 28 show the spatial distribution of inferred surficial geology, depth to bedrock, and ground ice information for the boreholes drilled around the Jericho Diamond Mine site, with similar figures for other mine sites provided in Appendix E.

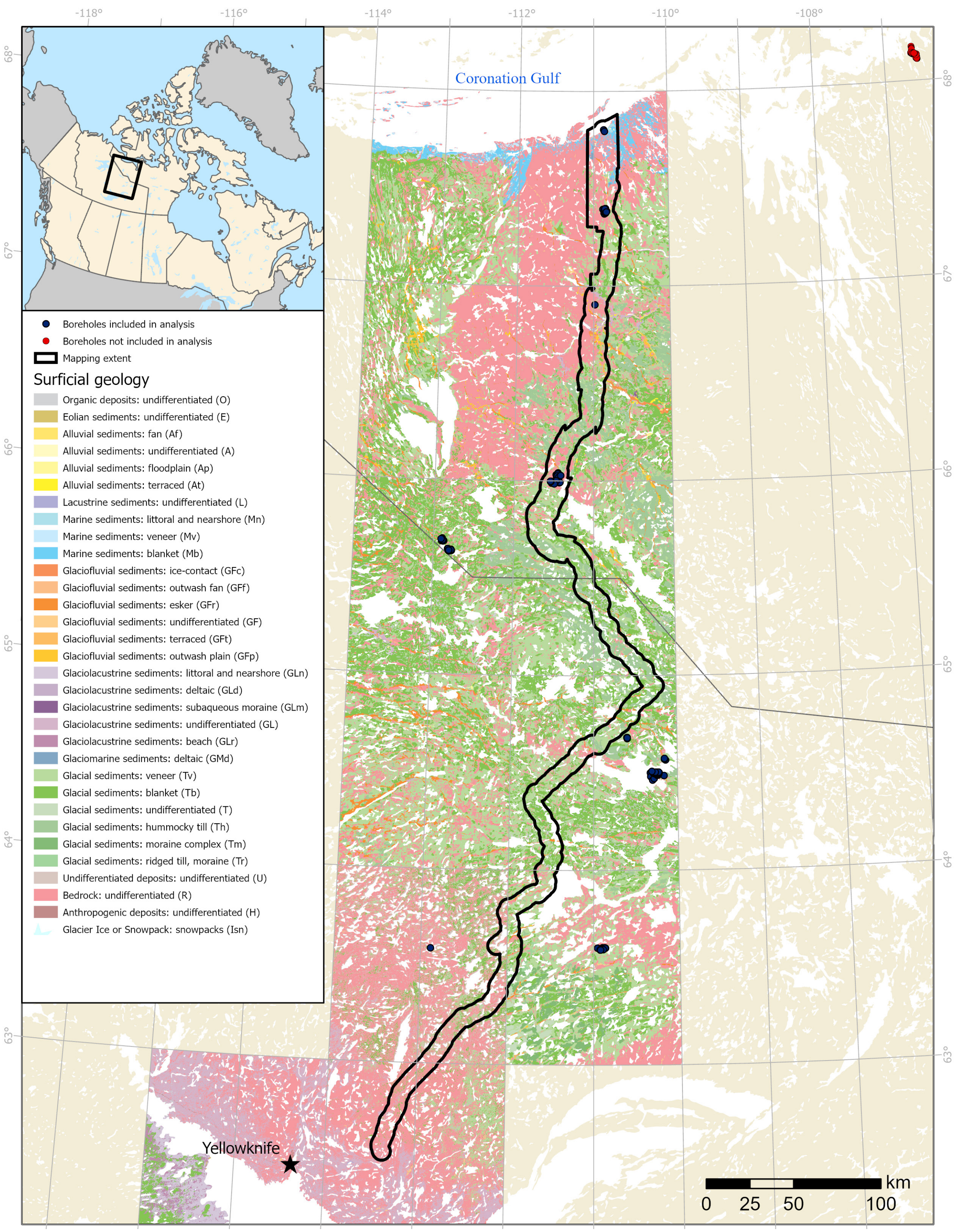

Figure 15: Geotechnical borehole locations.

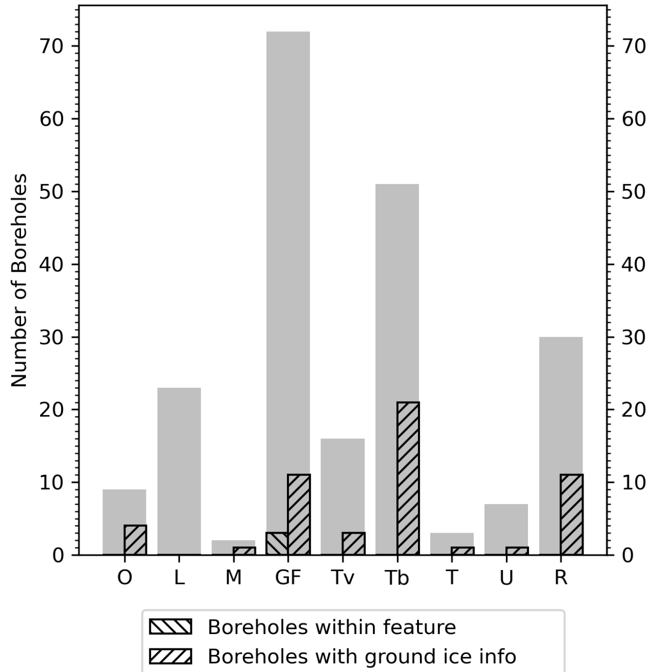

Figure 16. Counts of geotechnical boreholes in the region surrounding the mapping area according to surficial geology. Crosshatching denotes the number of boreholes within a digitized geomorphic feature (left) or with ground ice information (right). Surficial geology class codes follow those in Figures 9 and 10.

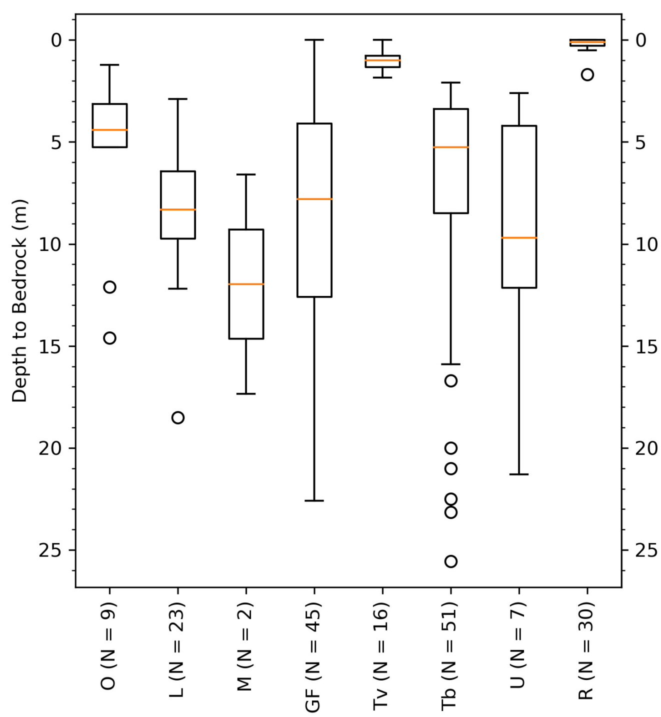

Figure 17. Boxplots of depth to bedrock measurements according to surficial geology for boreholes in the region surrounding the mapping area. Horizontal lines, boxes, whiskers, and circles denote the sample median, interquartile range, minimum and maximum, and outliers, respectively.

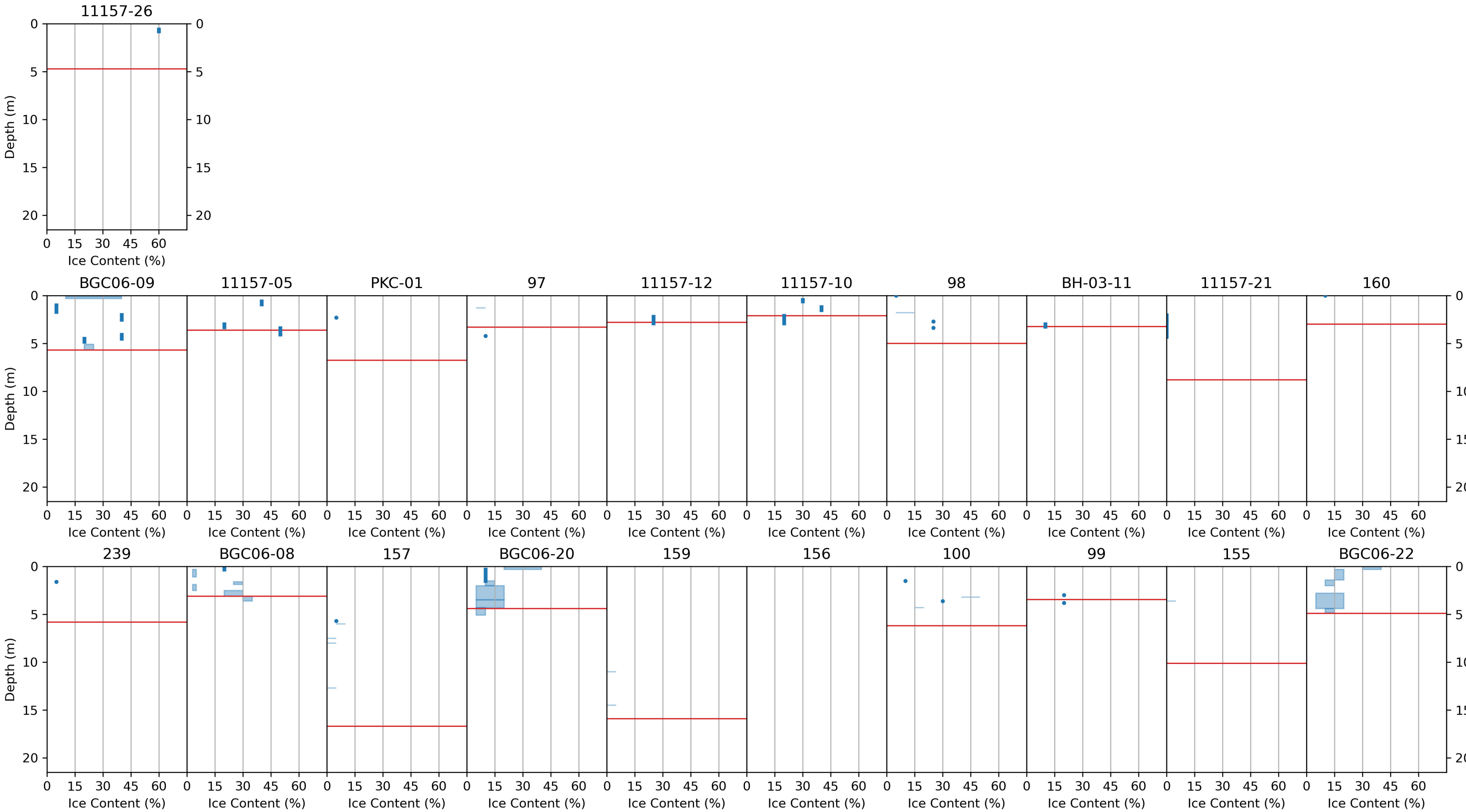

Figure 18. Visible ground ice contents reported for the boreholes drilled within till blanket glacial sediments (Tb). A box denotes visible ground ice content reported as a range over the depth interval. A solid vertical bar indicates that only one value was reported over the depth interval. A dot indicates that a single value was reported at a specific depth. The horizontal red lines represent the depth to bedrock where this information is available.

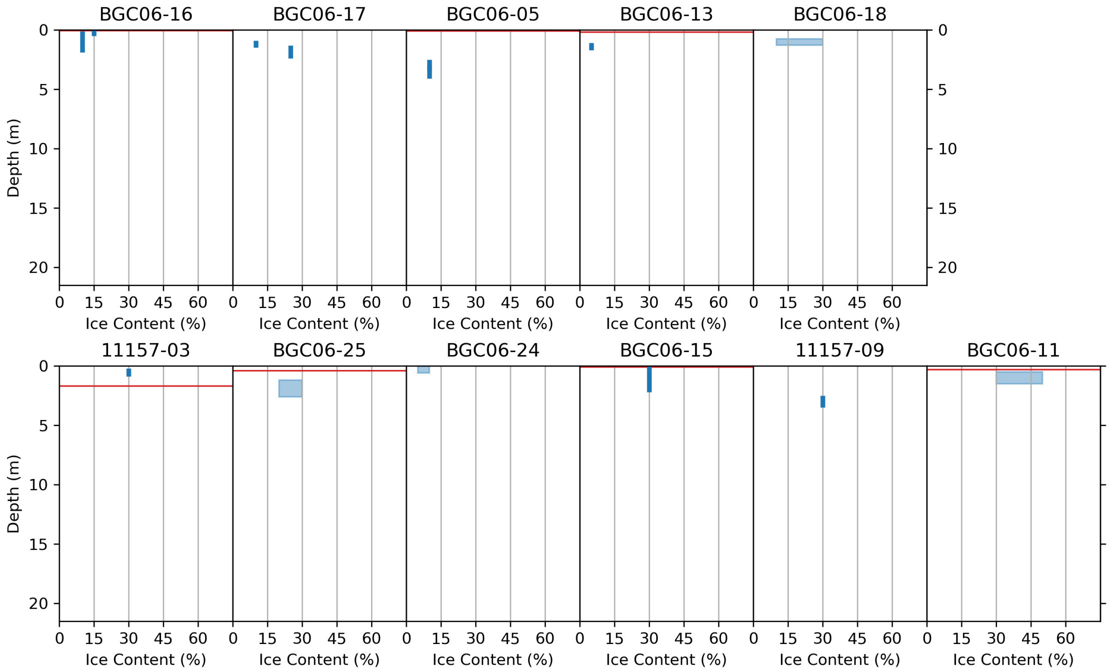

Figure 19. Visible ground ice contents reported for the boreholes drilled within bedrock (R). A box denotes visible ground ice content reported as a range over the depth interval. A solid vertical bar indicates that only one value was reported over the depth interval. A dot indicates that a single value was reported at a specific depth. The horizontal red lines represent the depth of bedrock information where available.

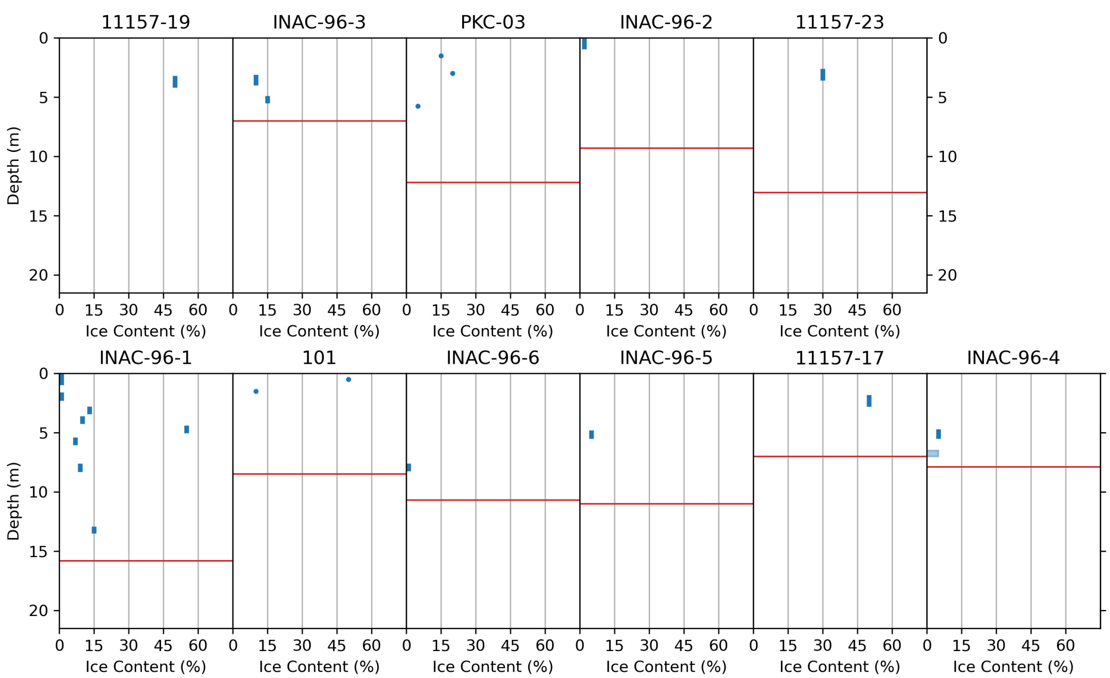

Figure 20. Visible ground ice contents reported for the boreholes drilled within undifferentiated glaciofluvial sediments (GF). A box denotes visible ground ice content reported as a range over the depth interval. A solid vertical bar indicates that only one value was reported over the depth interval. A dot indicates that a single value was reported at a specific depth. The horizontal red lines represent the depth of bedrock information where available.

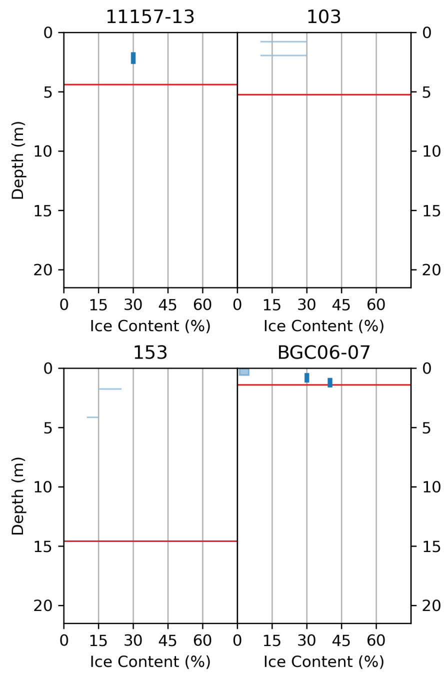

Figure 21. Visible ground ice contents reported for the boreholes drilled within organic deposits (O). A box denotes visible ground ice content reported as a range over the depth interval. A solid vertical bar indicates that only one value was reported over the depth interval. A dot indicates that a single value was reported at a specific depth. The horizontal red lines represent the depth of bedrock information where available.

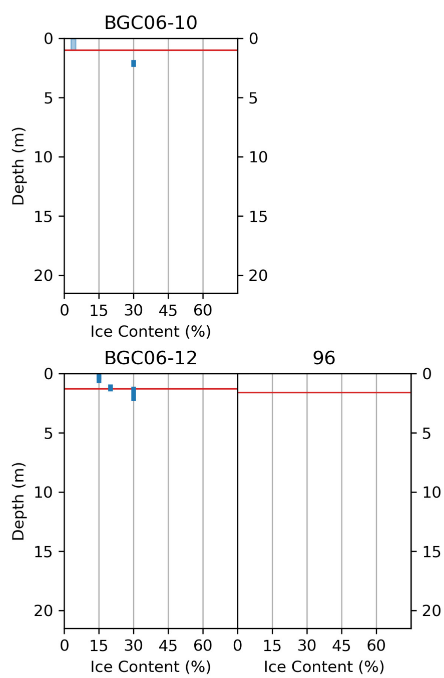

Figure 22. Visible ground ice contents reported for the boreholes drilled within glacial veneer sediments (Tv). A box denotes visible ground ice content reported as a range over the depth interval. A solid vertical bar indicates that only one value was reported over the depth interval. A dot indicates that a single value was reported at a specific depth. The horizontal red lines represent the depth of bedrock information where available.

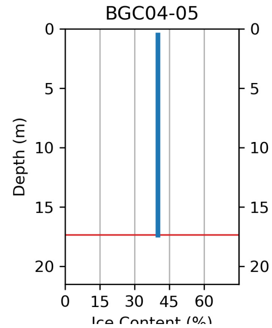

Figure 23: Visible ground ice contents reported for the boreholes drilled within undifferentiated marine sediments (M). A box denotes visible ground ice content reported as a range over the depth interval. A solid vertical bar indicates that only one value was reported over the depth interval. A dot indicates that a single value was reported at a specific depth. The horizontal red lines represent the depth of bedrock information where available.

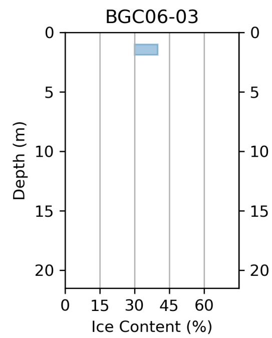

Figure 24: Visible ground ice contents reported for the boreholes drilled within undifferentiated glacial sediments (T). A box denotes visible ground ice content reported as a range over the depth interval. A solid vertical bar indicates that only one value was reported over the depth interval. A dot indicates that a single value was reported at a specific depth. The horizontal red lines represent the depth of bedrock information where available.

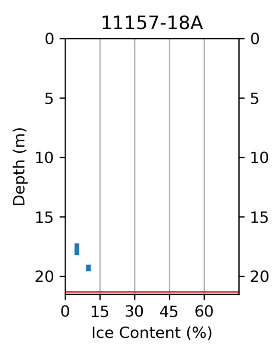

Figure 25: Visible ground ice contents reported for the boreholes drilled within undifferentiated sediments (U). A box denotes visible ground ice content reported as a range over the depth interval. A solid vertical bar indicates that only one value was reported over the depth interval. A dot indicates that a single value was reported at a specific depth. The horizontal red lines represent the depth of bedrock information where available.

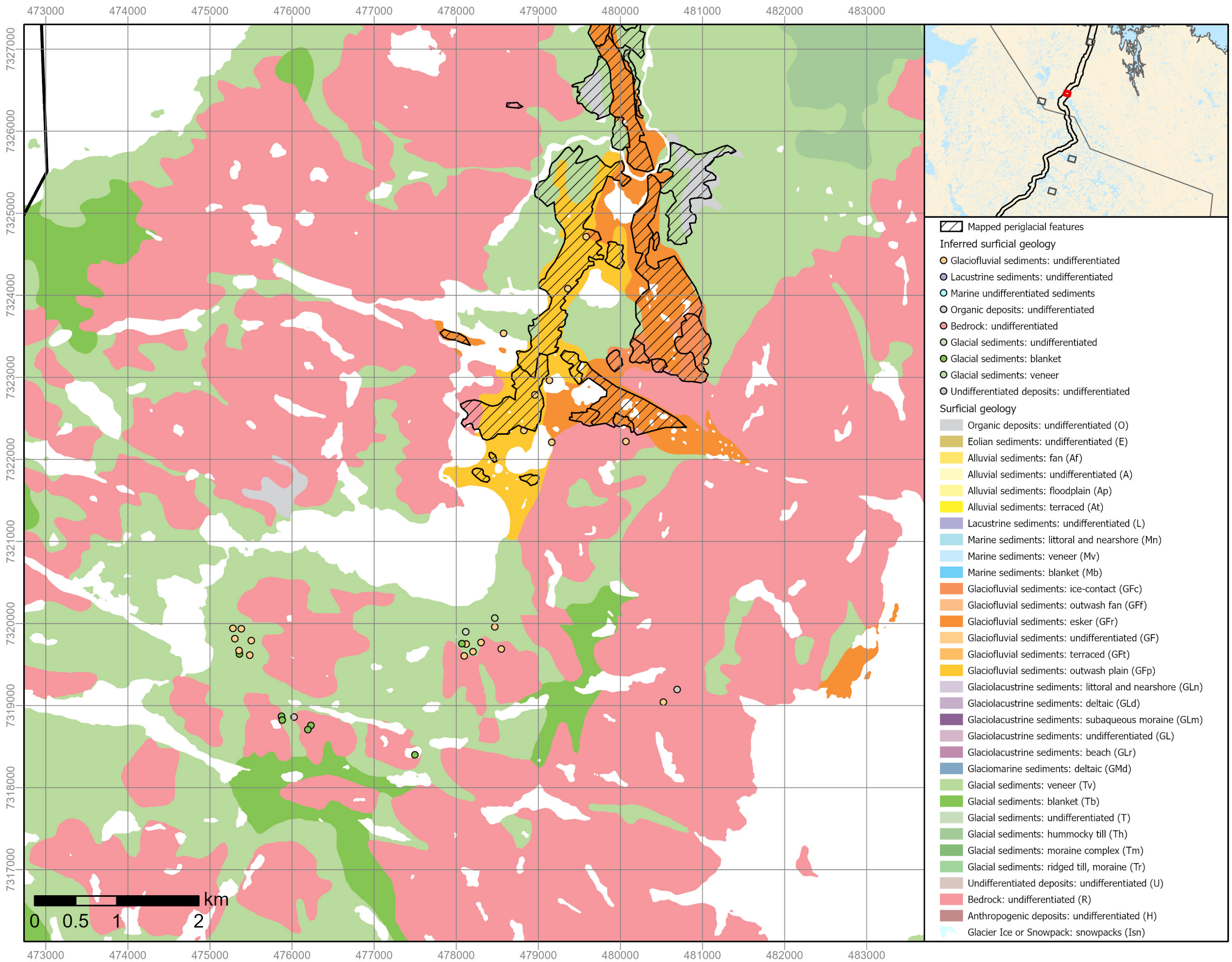

Figure 26: Inferred surficial geology for boreholes around the closed Jericho Diamond Mine site.

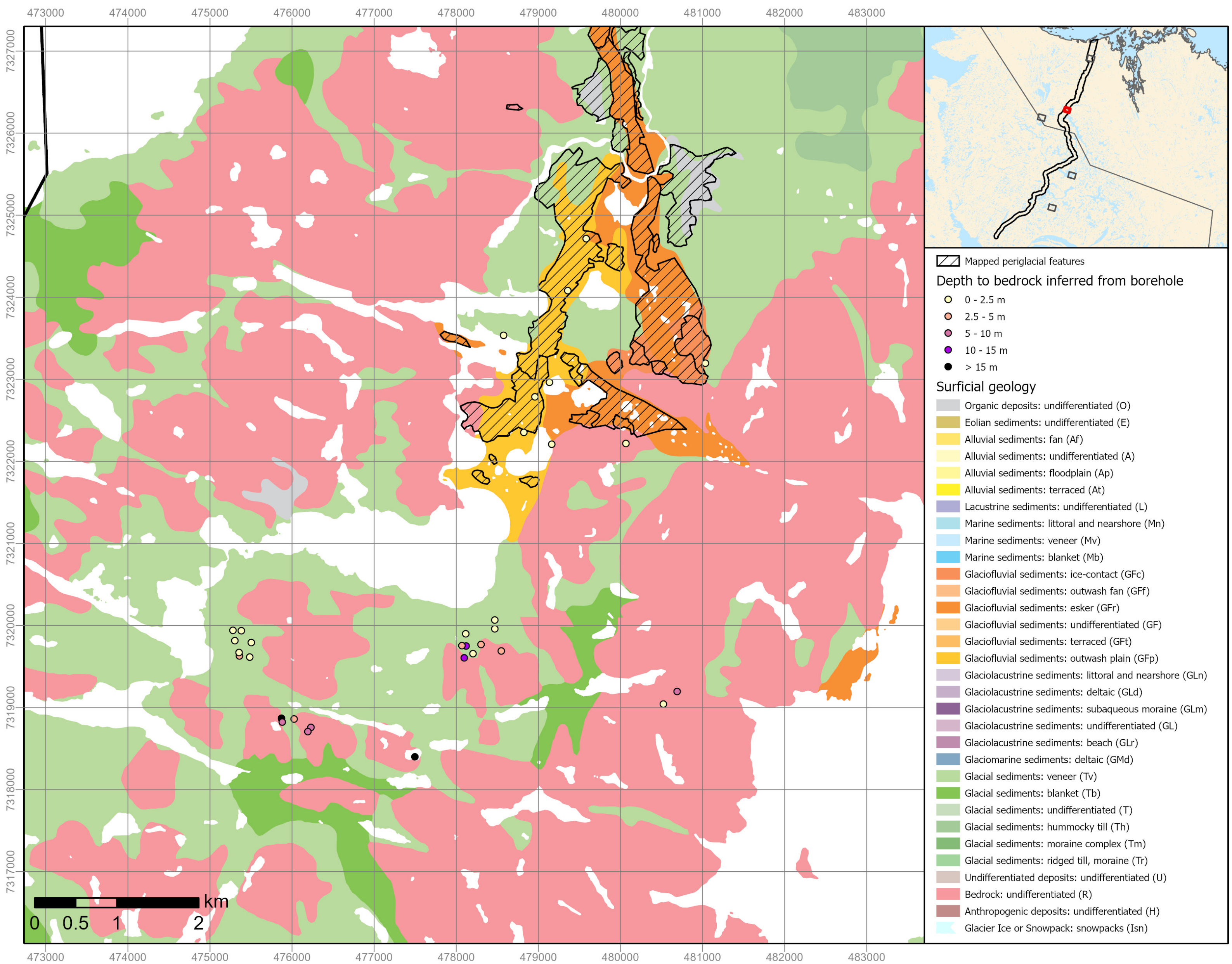

Figure 27: Depth to bedrock in boreholes around the closed Jericho Diamond Mine site.

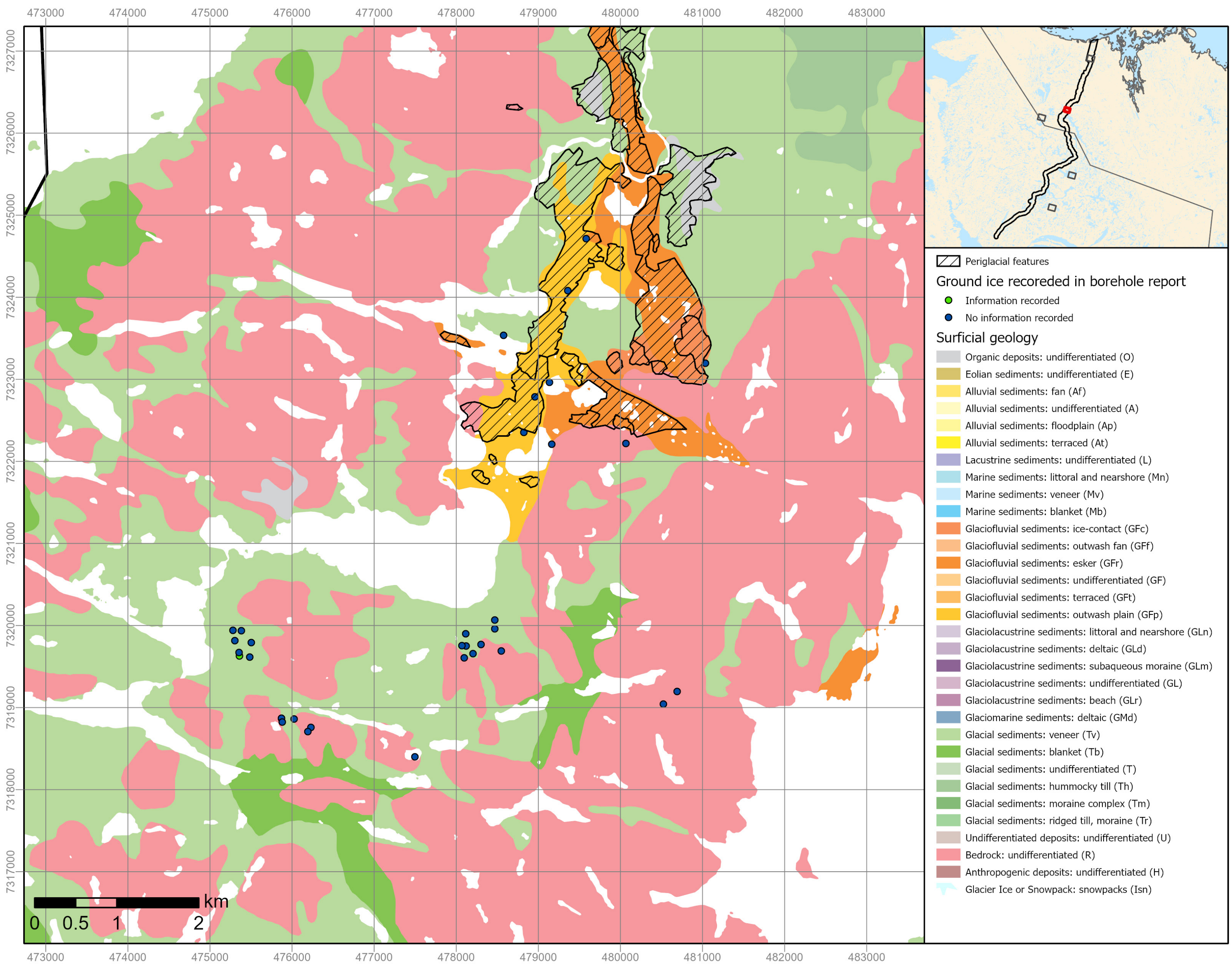

Figure 28: Ground ice data availability in boreholes around the closed Jericho Diamond Mine site.

4.3 Granular Deposits

A total of 2243 granular deposits (including 542 point features) and 40 geotechnical test pits were compiled (Figure 29). Within the analysis subset there are 27 geotechnical test pit samples, 22 granular deposit point features and 307 granular deposit point features. According to the point locations in the surficial geology data, geotechnical test pit samples taken within glaciofluvial esker sediments were the most numerous (24 samples) and showed a mean moisture content of 2.7% (Table 7) and a mean particle distribution of approximately 35% gravel, 63% sand, and 2% silt and clay. The three geotechnical test pit samples taken within undifferentiated glaciofluvial sediment units have a mean moisture content of 1.8% and a mean particle distribution of approximately 21% gravel, 78% sand, and 1% silt and clay. Table 8 and Table 9 show a matrix of deposit point features cross-referenced to inferred surficial geology units.

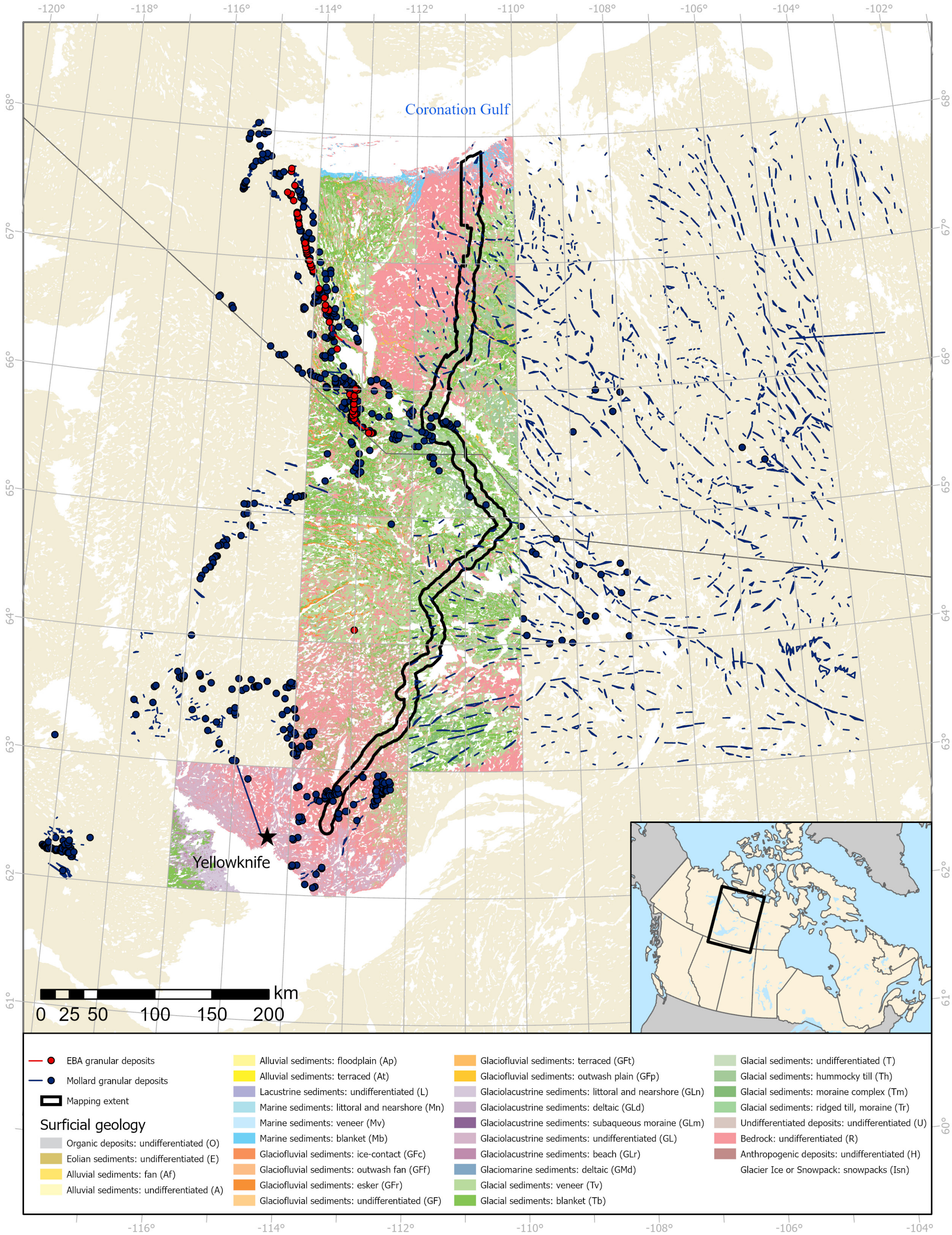

Figure 29. Granular deposit locations.

Table 7. Summary of the test pit data within the analysis region prepared by EBA Engineering and Consultants Ltd. (1993b).

Surficial geology	Number of samples	Mean moisture content (%)	Mean percentage passing through a 5 mm sieve (%)	Mean percentage passing through a 0.08 mm sieve (%)
GF	3	1.8	78.77	0.77
GFr	24	2.7	65.25	1.94

Table 8. Correlation matrix of the inferred surficial geology units and the granular deposit descriptions within the analysis region prepared by EBA Engineering and Consultants Ltd. (1993b).

Inferred surficial geology	Granular deposit description			Total
	Esker	Esker/ kame	Outwash	
GF	0	1	9	10
GFr	12	0	0	12
Total	12	1	9	22

Table 9. Correlation matrix of the inferred surficial geology units and the granular deposit descriptions within the analysis region prepared by J. D. Mollard and Associates Ltd. (1994, 1993).

Inferred surficial geology	Granular deposit description														Total
	No data	Delta	Esker	Esker/ delta	Esker/ kame	Esker/ kame/ outwash	Esker/ kame/ outwash /ice-contact deposit	Esker/ outwash	Ice-contact deposit	Kame	Kame/ outwash	Outwash	Outwash/ delta	Outwash/ ice-contact deposit	
GF	0	0	0	3	32	8	1	10	0	0	2	132	4	17	209
GFc	0	0	0	0	0	0	0	0	24	0	0	0	0	0	24
GFk	0	0	0	0	0	0	0	0	0	5	0	0	0	0	5
GFr	0	0	59	0	0	0	0	0	0	0	0	0	0	0	59
Lr	6	0	0	0	0	0	0	0	0	0	0	0	0	0	6
U	3	1	0	0	0	0	0	0	0	0	0	0	0	0	4
Total	9	1	59	3	32	8	1	10	24	5	2	132	4	17	307

5 Limitations

The geomorphic feature mapping follows the methods described by Sladen et al. (2021) and has similar limitations. The identification of landscape features relied heavily on digital and optical datasets with limited field validation. Some sections of the imagery did contain cloud cover that preventing mapping. However, there was often an overlapping cloud free image that could be used, so it is unlikely that cloud cover substantively affected the overall results. As mentioned previously the conclusions that can be drawn from the surficial geology attribute of the geomorphic features database are limited. This is due to the scale at which the surficial geology layers are published and the attribution of surficial geology according to the centroid of the mapped feature. An obvious consequence of this issue is the attribution bedrock to mapped features and compiled granular deposits and borehole data. We attempted to overcome this by analyzing the data with respect to the overlapping areas between features and surficial geology polygons, but without any other surficial geology data available to extract the attribute from, the attributes according to the centroids remain in the dataset.

The borehole and granular deposit compilation is limited to the publicly available publications that could be identified and compiled at the present time. The effort to compile additional resources is ongoing, and the compilation will be updated as more data is compiled. Borehole and granular deposit positions are based on locations reported in source files, but these have not been subsequently verified so may be incorrect. Another limitation from the methods used to extract information. Manual digitization and OCR are not perfect, and mistakes can occur. For manual digitization, errors can occur during data extraction and transfer to the database. The algorithm used for OCR can misidentify a character due to the low-quality scan of the documents. Each entry was manually checked over to mitigate the possibility of these errors occurring, however it should be noted that such errors may be present.

6 Summary

The data presented in this report is the result of a preliminary effort to provide: i) the first quantitative measures of the distributions and densities of various permafrost-related landforms in the vicinity of the proposed Grays Bay Road and Port Project corridor; and ii) a compilation of the geotechnical data of the surrounding region that we have located thus far that were not already available in digital form.

Within the mapping area 1291 periglacial features, 88 hydrological features, and 14 mass movement features have been identified and digitized. A total of 254 boreholes were compiled with 213 within the mapping area that were analyzed with respect to surficial geology. A total of 2243 granular deposits were compiled, and of the subset of points that fall within the map-sheets intersected by the study corridor there are 27 geotechnical test pit point features and 329 granular deposit point features.

Spatial analysis of the geomorphic feature data showed that the distributions and densities of the mapped permafrost-related landforms relate to surficial geology, with the highest counts of mapped features occurring within glacial, organic, and glaciofluvial deposits, though feature densities are highest in snowpack, eolian, marine littoral and nearshore, glaciolacustrine, and glaciofluvial deposits. Creep of frozen ground (which indicates the presence of ice-rich permafrost) occurs almost exclusively within glaciofluvial deposits, and for esker deposits it affects about 30% of the unit. The results of this study provide further evidence that high ground ice contents may be quite common in glaciofluvial deposits in this region and more extensive than the available geotechnical data indicate.

Analysis of the borehole data demonstrated that visible ground ice contents are typically between 10% and 30% visible ice, but are up to 55% in undifferentiated glaciofluvial and 60% in till blanket surficial geology units. Overburden thicknesses ranged up to approximately 25.5 m and were greatest in glaciofluvial, till blanket, and marine sediments. The test pit and granular deposit data showed that the samples were predominately collected from glaciofluvial deposits with grains distributed predominantly among sands and gravels, which is to be expected given the reason the sites were examined.

7 Data

This multi-part Open File includes data for mapped geomorphic features and compiled geotechnical borehole presented as GIS-ready ESRI shapefiles, and data for granular deposits are presented in Excel databases and as GIS-ready ESRI shapefiles. The Python scripts used in Sladen et al. (2021) were updated for this work and have been provided in Appendix D and on GitHub (https://github.com/gsc-permafrost/FeatureAttributeGeneration).

8 Acknowledgements

This project was supported by Natural Resources Canada (Climate Change Geoscience Program and the GEM-GeoNorth Program) and Transport Canada. Photographs included in Figure 7 were part of a joint helicopter survey by Geological Survey of Canada and Northwest Territory Geological Survey with support from Polar Continental Shelf Project. The authors would like to thank Stephen Wolfe for discussion about the geomorphological expression of creep of frozen ground. Anne-Marie Leblanc provided thoughtful comments that improved the report. Jason Chartrand and Tanner Kyle digitized and compiled geotechnical borehole data.

9 References

AGRA Earth & Environmental Limited, 1998. Massive Ice Study in Granular Deposits, Phase 2 Study. Submitted to Indian and Northern Affairs Canada.

Associate Committee on Geotechnical Research, 1988. Glossary of permafrost and related ground-ice terms. National Research Council. https://doi.org/10.4224/20386561

BGC Engineering Inc., 2006a. 2004 Geotechnical Investigation Program High Lake Project NU. Wolfden Resources Inc. Submitted to Nunavut Impact Review Board November 2006.

BGC Engineering Inc., 2006b. 2004-2005 Geotechnical investigations report, High Lake Project NU. Wolfden Resources Inc. Submitted to Nunavut Impact Review Board, November 2006.

Bostock, H.S., 2014. Physiographic regions of Canada. Geological Survey of Canada 293408. https://doi.org/10.4095/293408

Crown-Indigenous Relations and Northern Affairs Canada (CIRNAC), Government of Nunavut (GN), Nunavut Tunngavik Incorporated (NTI), Canada-Nunavut Geoscience Office (CNGO), 2021. Nunavut Mineral Exploration, Mining, and Geoscience.

Deblonde, C., Cocking, R.B., Kerr, D.E., Campbell, J.E., Eagles, S., Everett, D., Huntley, D.H., Inglis, E., Parent, M., Plouffe, A., Robertson, L., Smith, I.R., Weatherston, A., 2018. Surficial Data Model: the science language of the integrated Geological Survey of Canada data model for surficial geology maps. Geological Survey of Canada Open File 8236. https://doi.org/10.4095/308178

Dredge, L.A., Kerr, D.E., Wolfe, S.A., 1999. Surficial materials and related ground ice conditions, Slave Province, N.W.T., Canada. Canadian Journal of Earth Sciences 36, 1227–1238. https://doi.org/10.1139/cjes-36-7-1227

EBA Engineering Consultants Ltd., 1998. 1997/1998 Geotechnical Site Investigation. Prepared for Diavik Diamonds Inc. (submitted for Environmental Impact Study).

EBA Engineering Consultants Ltd., 1997. Granular resource investigation Lac de Gras, NWT geotechnical report.

EBA Engineering Consultants Ltd., 1995a. Koala Mine airport esker evaluation.

EBA Engineering Consultants Ltd., 1995b. Esker research study sampling and testing of Lac de Gras area, NWT.

EBA Engineering Consultants Ltd., 1993a. Izok project feasibility study mine site geotechnical investigation.

EBA Engineering Consultants Ltd., 1993b. Izok project feasibility study mine site geotechnical investigation - 37668.

EBA Engineering Consultants Ltd., 1993c. Izok project feasibility study winter haul road.

Environment Canada, 2022. Canadian Climate Normals [WWW Document]. URL https://climate.weather.gc.ca/climate_normals/index_e.html (accessed 3.10.22).

Geological Survey of Canada, 2017a. Surficial geology, Kikerk Lake, Nunavut, NTS 86-P, Geological Survey of Canada, Canadian Geoscience Map. https://doi.org/10.4095/299206

Geological Survey of Canada, 2017b. Surficial geology, Hepburn Island, Nunavut, NTS 76-M, Geological Survey of Canada, Canadian Geoscience Map. https://doi.org/10.4095/299205

Geological Survey of Canada, 2016a. Surficial geology, Point Lake, Northwest Territories - Nunavut, NTS 86-H, Geological Survey of Canada, Canadian Geoscience Map. https://doi.org/10.4095/298703

Geological Survey of Canada, 2016b. Surficial geology, Napaktulik Lake, Nunavut, NTS 86-I, Geological Survey of Canada, Canadian Geoscience Map. https://doi.org/10.4095/298708

Geological Survey of Canada, 2015. Surficial geology, Winter Lake, Northwest Territories, NTS 86-A, Geological Survey of Canada, Canadian Geoscience Map. https://doi.org/10.4095/295588

Geological Survey of Canada, 2014a. Surficial geology, Lac de Gras, Northwest Territories, NTS 76-D, Geological Survey of Canada, Canadian Geoscience Map. https://doi.org/10.4095/295497

Geological Survey of Canada, 2014b. Surficial geology, Contwoyto Lake, Northwest Territories - Nunavut, NTS 76-E, Geological Survey of Canada, Canadian Geoscience Map. https://doi.org/10.4095/295192
Gibson, C., Morse, P.D., Kelly, J.M., Turetsky, M.R., Baltzer, J.L., Gingras-Hill, T., Kokelj, S. v, 2020. Thermokarst mapping collective: Protocol for organic permafrost terrain and preliminary inventory from the Taiga Plains test area, Northwest Territories. NWT Open Report 2020-010.
Golder Associates Ltd., 2001. Report on Snap Lake Diamond Project Surface Engineering Optimization Study Geotechnical Factual Report. Report No. 012-1436/5211 submitted to AMEC Simons Mining & Metals.
Heginbottom, J.A., Dubreuil, M.H., Harker, P.T., 1995. Canada, Permafrost. National Atlas of Canada. https://doi.org/10.4095/294672
Helmstaedt, H., 2009. Crust-mantle coupling revisited: The Archean Slave craton, NWT, Canada. Lithos 112, 1055–1068. https://doi.org/10.1016/j.lithos.2009.04.046
J.D. Mollard and Associates Ltd., 1994. Compilation inventory of granular material resources information bordered by latitude 63 and 68 and longitude 102 and112 in NWT.
J.D. Mollard and Associates Ltd., 1993. Compilation inventory of granular material resources information within the Izok Lake transportation corridor.
Kerr, D.E., 2018. Reconnaissance surficial geology, Kathawachaga Lake, Nunavut, NTS 76-L, Geological Survey of Canada, Canadian Geoscience Map. https://doi.org/10.4095/308367
Kerr, D.E., 2014. Reconnaissance surficial geology, MacKay Lake, Northwest Territories, NTS 75-M, Geological Survey of Canada, Canadian Geoscience Map. https://doi.org/10.4095/295542
Kerr, D.E., 1996. Late Quaternary sea level history in the Paulatuk to Bathurst Inlet area, Northwest Territories. Canadian Journal of Earth Sciences 33, 389–403. https://doi.org/10.1139/e96-029
Mackay, J.R., 2000. Thermally induced movements in ice-wedge polygons, western arctic coast: A long-term study. Geographie Physique et Quaternaire 54, 41–68. https://doi.org/10.7202/004846ar
Natural Resources Canada, 2016. The UTM Grid - Military Grid Reference System [WWW Document]. URL https://www.nrcan.gc.ca/earth-sciences/geography/topographic-information/maps/utm-grid-map-projections/utm-grid-military-grid-reference-system/9789 (accessed 3.13.22).
Natural Resources Canada, 2021. CanVec.
Olthof, I., Kerr, D.E., Wolfe, S.A., Eagles, S., 2014. Predictive surficial materials and surficial geology from LANDSAT-7, Upper Carp Lake, NTS 85-P, Northwest Territories., Geological Survey of Canada, Open File 7601. https://doi.org/10.4095/293970
O'Neill, H.B., Duchesne, C., Jardine, S., Smith, S.L., n.d. Permafrost Information Network (PIN) Geotechnical Borehole Database (beta) [WWW Document]. URL https://pin.geosciences.ca/docs/PIN_db_metadata and field descriptions_Dec2018.pdf
O'Neill, H.B., Wolfe, S.A., Duchesne, C., 2020. Ground ice map of Canada. Geological Survey of Canada Open File 8713. https://doi.org/10.4095/326885
Padgham, W.A., Fyson, W.K., 1992. The Slave Province: a distinct Archean craton. Canadian Journal of Earth Sciences 29, 2072–2086. https://doi.org/10.1139/e92-165
Porter, C., Morin, P., Howat, I., Noh, M.-J., Bates, B., Peterman, K., Keesey, S., Schlenk, M., Gardiner, J., Tomko, K., Willis, M., Kelleher, C., Cloutier, M., Husby, E., Foga, S., Nakamura, H., Platson, M., Wethington Jr., M., Williamson, C., Bauer, G., Enos, J., Arnold, G., Kramer, W., Becker, P., Doshi, A., D'Souza, C., Cummens, P., Laurier, F., Bojesen, M., 2018. ArcticDEM. https://doi.org/10.7910/DVN/OHHUKH
Sladen, W.E., Parker, R.J.H., Kokelj, S.V., Morse, P.D., 2021. Geomorphologic feature mapping methodology developed for the Dempster Highway and Inuvik-to-Tuktoyaktuk Highway

corridors. Geological Survey of Canada Open File 8751. https://doi.org/https://doi.org/10.4095/328181
Smith, S.L., Burgess, M.M., Chartrand, J., Lawrence, D.E., 2005. Digital borehole geotechnical database for the Mackenzie Valley/Delta region. Geological Survey of Canada Open File 4924.
SRK Consulting Engineers and Scientists, 2005. Preliminary surface infrastructure design, Doris North Project, Hope Bay Nunavut Canada. Prepared for Miramar Hope Bay Ltd. Submitted to Nunavut Impact Review Board 2005.
SRK Consulting Engineers and Scientists, 2003. Supplemental Geotechnical Data, Jericho project Nunavut. Report prepared for Tahera Corp. Technical Memorandum A in Environmental Impact Study submitted to Nunavut Impact Review Board.
SRK Consulting Engineers and Scientists, 2002. Hope Bay Doris North Project. Tail Lake dam site geotechnical investigation and conceptual design report, Nunavut Canada. Prepared for Miramar Hope Bay Limited, Dec. 2002. Submitted to Nunavut Impact Review Board 2005.
Stevens, C.W., Kerr, D.E., Wolfe, S.A., Eagles, S., 2017. Predictive surficial geology, Yellowknife and Hearne Lake, Northwest Territories, NTS 85-J and 85-I, Geological Survey of Canada, Canadian Geoscience Map. https://doi.org/10.4095/299516
Wolfe, S.A., Burgess, M.M., Douma, M., Hyde, C., Robinson, S., 1997. Geological and geophysical investigations of massive ground ice in glaciofluvial deposits, Slave Geological Province, Northwest Territories. Geological Survey of Canada Open File 3442. https://doi.org/10.4095/208917
Wolfe, S.A., Kerr, D.E., Morse, P.D., 2017. Slave Geological Province: An Archetype of Glaciated Shield Terrain, in: Landscapes and Landforms of Western Canada. pp. 77–86. https://doi.org/10.1007/978-3-319-44595-3_4
Zoltai, S.C., 1993. Cyclic development of permafrost in the peatlands of Northwestern Alberta, Canada. Arctic and Alpine Research 25, 240–246.
Zoltai, S.C., Tarnocai, C., 1975. Perennially frozen peatlands in the Western Arctic and subarctic of Canada. Canadian Journal or Earth Sciences 28–43.